frontiers in Immunology

ORIGINAL RESEARCH
published: 22 December 2017
doi: 10.3389/fimmu.2017.01868

# Abnormal Complement Activation and Inflammation in the Pathogenesis of Retinopathy of Prematurity

*Sonika Rathi[1], Subhadra Jalali[2], Satish Patnaik[1], Shahna Shahulhameed[1], Ganeswara R. Musada[1], Divya Balakrishnan[2], Padmaja K. Rani[2], Ramesh Kekunnaya[3], Preeti Patil Chhablani[3], Sarpras Swain[4], Lopamudra Giri[4], Subhabrata Chakrabarti[1] and Inderjeet Kaur[1]**

[1] Prof Brien Holden Eye Research Centre, Hyderabad, India, [2] Smt. Kanuri Santhamma Centre for Vitreo Retinal Diseases, Hyderabad, India, [3] Jasti V Ramanamma Children's Eye Care Centre, L V Prasad Eye Institute, Hyderabad, India, [4] Indian Institute of Technology, Hyderabad, India

OPEN ACCESS

**Edited by:**
*Uday Kishore, Brunel University London, United Kingdom*

**Reviewed by:**
*Taruna Madan, National Institute for Research in Reproductive Health (ICMR), India*
*Lubka T. Roumenina, INSERM UMRS1138 Centre de Recherche des Cordeliers, France*

***Correspondence:**
*Inderjeet Kaur*
*inderjeet@lvpei.org, ikaurs@gmail.com*

**Specialty section:**
*This article was submitted to Molecular Innate Immunity, a section of the journal Frontiers in Immunology*

**Received:** *02 October 2017*
**Accepted:** *08 December 2017*
**Published:** *22 December 2017*

**Citation:**
*Rathi S, Jalali S, Patnaik S, Shahulhameed S, Musada GR, Balakrishnan D, Rani PK, Kekunnaya R, Chhablani PP, Swain S, Giri L, Chakrabarti S and Kaur I (2017) Abnormal Complement Activation and Inflammation in the Pathogenesis of Retinopathy of Prematurity. Front. Immunol. 8:1868. doi: 10.3389/fimmu.2017.01868*

Retinopathy of prematurity (ROP) is a neurovascular complication in preterm babies, leading to severe visual impairment, but the underlying mechanisms are yet unclear. The present study aimed at unraveling the molecular mechanisms underlying the pathogenesis of ROP. A comprehensive screening of candidate genes in preterms with ROP ($n = 189$) and no-ROP ($n = 167$) was undertaken to identify variants conferring disease susceptibility. Allele and genotype frequencies, linkage disequilibrium and haplotypes were analyzed to identify the ROP-associated variants. Variants in *CFH* ($p = 2.94 \times 10^{-7}$), *CFB* ($p = 1.71 \times 10^{-5}$), *FBLN5* ($p = 9.2 \times 10^{-4}$), *CETP* ($p = 2.99 \times 10^{-5}$), and *CXCR4* ($p = 1.32 \times 10^{-8}$) genes exhibited significant associations with ROP. Further, a quantitative assessment of 27 candidate proteins and cytokines in the vitreous and tear samples of babies with severe ROP ($n = 30$) and congenital cataract ($n = 30$) was undertaken by multiplex bead arrays and further validated by western blotting and zymography. Significant elevation and activation of MMP9 ($p = 0.038$), CFH ($p = 2.24 \times 10^{-5}$), C3 ($p = 0.05$), C4 ($p = 0.001$), IL-1ra ($p = 0.0019$), vascular endothelial growth factor (VEGF) ($p = 0.0027$), and G-CSF ($p = 0.0099$) proteins were observed in the vitreous of ROP babies suggesting an increased inflammation under hypoxic condition. Along with inflammatory markers, activated macrophage/microglia were also detected in the vitreous of ROP babies that secreted complement component C3, VEGF, IL-1ra, and MMP-9 under hypoxic stress in a cell culture model. Increased expression of the inflammatory markers like the IL-1ra ($p = 0.014$), MMP2 ($p = 0.0085$), and MMP-9 ($p = 0.03$) in the tears of babies at different stages of ROP further demonstrated their potential role in disease progression. Based on these findings, we conclude that increased complement activation in the retina/vitreous in turn activated microglia leading to increased inflammation. A quantitative assessment of inflammatory markers in tears could help in early prediction of ROP progression and facilitate effective management of the disease, thereby preventing visual impairment.

**Keywords: retina, premature birth, inflammation, genetics, cytokines, abnormal angiogenesis, microglia/macrophage, alternative complement pathway**

## INTRODUCTION

Retinopathy of prematurity (ROP) is a complex disease of the retina with a multi-factorial etiology and an early intervention has been observed to prevent irreversible vision loss in some of these prematurely born infants (1). Its incidence in developed countries with adequate neonatological facilities (like United States) is 19.88% (2) while it is slightly higher (~30%) for middle-income developing countries (3, 4). In India, approx. two million babies are at risk of developing ROP annually (4) with an overall incidence estimated to be around 45% (5, 6). Hence, ROP is one of the major causes of visual impairment in India. Lower gestational age (GA), lower birth weight (BW), and oxygen supplementation are the primary risk factors associated with ROP (7). It is a self-limiting disease with initial symptoms of avascular retina that progresses to abnormal growth of retinal vessels causing retinal detachment (8). Hypoxia in the avascular retina is considered to be the primary cause for neovascularization in ROP that further activates various cellular pathways such as HIF1α, eNOS/iNOS, and vascular endothelial growth factor (VEGF) signaling leading to abnormal neovascularization (9, 10). However, the detailed molecular mechanisms underlying neovascularization in ROP have not been elucidated yet. So far, few functionally relevant genes (*NDP, FZD4, LRP5, CFH, VEGF, ANGPT2, EPO, BDNF,* and *CETP*) have been associated with ROP in a small fraction of cases. But, many of these variants could not be replicated across different ethnicities (11–13). Further, their roles in risk predictions and disease management are yet to be determined.

The protein profiles in the vitreous have been utilized for studying the underlying pathology of the retina due to its proximity. This has largely been accomplished by analyzing the levels of erythropoietin, VEGF, and cytokines like interleukins (IL-6, IL-7, IL-10, and IL-15), Eotaxin, FGF basic, G-CSF, GM-CSF, IP-10, and RANTES in the vitreous to identify their potential as biomarkers for ROP progression (14–16). Interestingly, interleukin-7 (IL-7), monocyte chemotactic protein-1, and macrophage inflammatory protein 1 (MIP-1α and MIP-1β) levels were also found to be significantly elevated in the cord blood serum of ROP (17). Earlier, low serum levels of IGF-1 and VEGF were reported in preterm babies with severe ROP and low GA (18, 19). Thus, the studies on protein profiling and genetic associations of ROP could explain the susceptibility of some preterm babies progressing to severe ROP.

Our study is an attempt to comprehensively elucidate the genomic basis of ROP and identify the potential biomarkers for progression to severe stages. Since, no mutations were observed in the Norrin signaling genes in ROP in our earlier study (20), we explored genes involved in angiogenesis, growth, and development of the fetal retina, trans-endothelial migration, oxidative stress, inflammation, and neurodegenerative processes, in order to understand their role in ROP pathogenesis. We observed strong associations of ROP with the variants in *CFH*, *CFB, CXCR4, FBLN5,* and *CETP* genes along with increased levels of proteins in the extracellular matrix (ECM) and complement pathways in the vitreous of these babies. We observed the presence of the activated microglia/macrophages in the retina and vitreous. We further demonstrated the activated microglial cells under hypoxia expressed complement C3, VEGF, and IL-1β, thereby resulting in abnormal blood vessel proliferation in the ROP-affected eyes. We also evaluated the inflammatory proteins as potential biomarkers for ROP based on their expressions in the tear samples of the ROP patients.

## MATERIALS AND METHODS

### Study Subjects

The study protocol adhered to the tenets of declaration of Helsinki and was approved by the Institutional Review Board (LEC02-14-029) of the L V Prasad Eye Institute (LVPEI). Preterm babies referred for further management from the neonatal intensive care units of different hospitals in Hyderabad to the LVPEI between January 2007 and December 2010 were enrolled. Overall, the study cohort comprised 372 preterm babies of GA $\leq$ 35 weeks and/or BW $\leq$ 1,700 g with ROP ($n = 189$) and no-ROP ($n = 167$). A detailed demographic and clinical history (Table S1 in Supplementary Material) of all the preterm babies enrolled were documented and a written informed consent was obtained from their parents. The diagnosis and categorization of ROP cases from mild to severe form was based on severity (stages 1–5), location (zones I, II, III), amount of disease (clock hours), and presence or absence of "plus" disease following ICROP guidelines (20, 21) (Figure S2 in Supplementary Material). Severe ROP includes progressive disease, which requires prompt treatment. It includes any stage (1–5) Zone I with plus and stages 2–3 Zone II with plus. Mild ROP cases include less severe disease, which does not require any treatment. Although until the regression of the disease completely, babies are under regular follow-up for ROP screening.

### Sample Collection

Venous blood (0.5–1 mL) was collected from the ROP and no-ROP preterm babies by venipuncture. DNA was extracted from the blood samples using an automated DNA extraction platform (MagNa Pure LC 20, Roche) following the manufacturers guidelines. Likewise, for proteomic studies, the vitreous humor samples (100–500 μL) were collected from preterm babies with stage IV and V ROP ($n = 30$) who had undergone vitrectomy as a part of their routine clinical management. The controls for the proteomic studies included babies with congenital cataract (<6 months of age) who underwent partial vitrectomy as part of the surgical management ($n = 30$). The vitreous samples were immediately centrifuged at relative centrifugal force (rcf) of 10,621 g and the supernatant was stored at −80°C deep freezer until further use.

Additionally, crude tears were collected before instilling any drops or drug for pupil dilation in the eyes of preterm babies with ROP (Stage II–V) ($n = 27$) and no-ROP ($n = 13$) using a capillary tube and without touching the conjunctiva. The tear samples for ROP subjects were collected during the active disease condition either before or after 3 months following medical intervention.

### Customized Genotyping of Candidate Variants

A customized panel containing 384 single-nucleotide polymorphisms (SNPs) from 26 chosen genes (Table S2 in Supplementary

Material) involved in growth and development of the fetal retina, angiogenesis, inflammation, neurodegeneration, and oxidative stress processes were genotyped using a microarray platform (Illumina Inc., golden gate assay). Following hybridization, the fluorescent signals were scanned by a bead array reader and the raw signal intensities were imported to the Genome Studio software (version 1.9) for assessing quality scores. The assay and sample reliability were measured by means of the gen call score and the genotypes were called following clustering. The genotypes of a subset of samples for all the genes were validated by resequencing on an automated DNA sequencer (ABI 3130 XL) using the BigDye chemistry.

## Quantitative Assessment of Cytokines and Other Proteins in the Vitreous and Tear Samples

The concentrations of 27 cytokines (Bio-Plex Human cytokine 27-Plex, Bio-Rad, Hercules, CA, USA) and 28 different proteins (HMMP1-55K, HMMP2-55K, HNDG1-36K, HNDG2-36K, HTIMP2-54K, TGFB-64K-03, HYCYTOMAG-60K, Merck Millipore, Billerica, MA, USA) involved in ECM remodeling, angiogenesis and inflammatory pathways were screened by multiplex bead immunoassays using the Luminex xMAP technology in vitreous samples that were pre-diluted to concentration 1:3. Similar assay was used for estimating the concentrations of MMPs and cytokines in the tears samples and were quantitated by comparing them with their respective standard curve. All standards and some of the samples (due to less volume of samples) were measured in duplicates.

## Validation of the Differentially Regulated Proteins by Western Blotting and Zymography

A part of vitreous sample (50–100 μL) was lysed using a buffer containing 50 mM Tris-HCl (pH = 8), 120 mM NaCl, 0.5% NP40, protease inhibitor cocktail, and precipitated with acetone. The protein pellet was eluted in 50 μL of 1× phosphate buffered saline (PBS) containing the protease inhibitor cocktail and quantified by bicinchoninic acid assay. The normalized vitreous proteins (10 μg) were then subjected to western blotting. Western blotting was done using mouse anti-human C3 antibody (sc-28294, Santa Cruz) and mouse anti-human C5 (MAB2037, R&D Systems) followed by incubation with IRDye® 680RD secondary antibody. The entire procedure was done according to the manufacturer's recommended application protocol (https://www.licor.com).

MMP gelatinase activity was measured in the vitreous and tear of ROP babies and controls by zymography as described earlier (22). An equal volume of crude vitreous and tear samples were electrophoresed under non-reducing conditions in 10% SDS-PAGE gels polymerized with 1 mg/mL gelatin. The gel was washed with 2.5% Triton X-100 for 30 minutes at room temperature with gentle agitation, followed by rinsing with distilled water. The gel was then incubated for 30 min in developing buffer containing 50 mM Tris-HCl, pH 7.8, 5 mM $CaCl_2$, 0.2 M NaCl, 0.02% Brij 35. The gel was incubated with fresh developing buffer at 37°C for 16 h and stained with Coomassie blue (Bio-Rad). This was followed by destaining with 10% v/v methanol, 5% v/v acetic acid in $dH_2O$. Active MMP (MMP2/MMP9) band was detected in the zymogram in the discovery cohort. The observations of discovery cohort were further validated in tears in an extended cohort of patients at different stages of ROP: no-ROP ($n = 9$), mild ROP regressed ($n = 6$), mild ROP_progressed ($n = 7$), and severe ROP ($n = 12$) by zymography in order to confirm their role as biomarker in ROP pathogenesis. Zymogram band intensities were calculated with ImageJ software.

## Immunohistochemistry and Hematoxylin and Eosin (H&E) Staining for Macrophage/Microglia in the Vitreous

Vitreous were subjected to cytospin to separate the cells that were embedded in the parafilm block. Sections were cut, air dried, and stained with H&E (23) for understanding their morphology. Tissue sections were then deparaffinized using xylene and gradually rehydrated with ethanol. Antigen retrieval was done by microwaving the sections at full power for 4–5 min in Tris EDTA buffer (10 mM Tris, 1 mM EDTA, 0.5% tween 20, pH 9.0). Blocking was carried out with 2.5% (w/v) BSA in PBS (10 mmol/L sodium phosphate, pH 7.5, 120 mmol/L sodium chloride) for 30 min at room temperature. Thereafter, the slides were incubated for 60 min with the primary antibody (CD 68 for human 1:100) diluted in 1× PBS, followed by three washings with PBS. Further incubation was carried out with biotinylated anti-mouse immunoglobulin. Sections were then washed in PBS and incubated with avidin DH/biotinylated horseradish peroxidase reagent in PBS for 30 min before final washing. The antigen was localized using 1 mg/mL diaminobenzidene tetrahydrochloride (DAB; Sigma), 0.2% $H_2O_2$ in 50 mmol/L Tris–HCl, pH 7.6, which appeared as a brown end product. Sections were then counter-stained with DAPI for nuclei staining.

## Response to Hypoxia by the Cultured Microglia Cells

The human microglial cell line (CHME3) was cultured in DMEM containing 10% FBS along with antibiotics penicillin and streptomycin. The confluent cells were trypsinized using 0.25% trypsin-EDTA. Hypoxic stress was introduced in the microglia cells by treating them with Cobalt chloride ($CoCl_2$) at various concentrations from 100 to 250 μm. Briefly, around 15,000 cells were seeded on a six well plate and then serum deprived for 6 h, followed by treatment with $CoCl_2$ for 24 h on attaining 70–80% confluency. The serum deprived cells in the same duration that were not treated for hypoxia were used as controls.

## $Ca^{2+}$ Staining and Live Cell Imaging

The cells were washed in HBSS (Thermoscientific, Waltham, MA, USA) and then incubated with the calcium binding dye Flu-4 (diluted with HBSS 1:750) for 30 min. After washing the cells with HBSS three times, live cell imaging was performed for 10 min using an EVOS fluorescent microscope (Thermo Fischer

Scientific, Waltham, MA, USA) under 20× magnification. The cytosolic calcium flux was measured using the change in Fluo-4 intensity over time for individual cells (Excitation: 494 nm Emission: 506 nm) (24).

## Semi-Quantitative PCR

The RNA from untreated and treated cells was extracted by Trizol method (25). The cDNA was prepared using iScript cDNA synthesis kit (Bio-Rad, CA, USA). Semi quantitative PCR was carried out using the specific primers (Table S3 in Supplementary Material) for *VEGF165*, *C3*, *HIF1*α, *BAX*, and *IL-1*β while β-*actin* was used as an endogenous control.

## Statistical and Bioinformatic Analysis

Allele frequencies of all the 384 variants were calculated by gene counting method along with odds ratio and 95% CI. A $p$ value $< 0.05$ was considered to be significant. The associated allele and haplotype frequencies were further analyzed for statistical correction using Bonferroni and permutations tests ($n = 10{,}000$ permutations). Estimates of Hardy–Weinberg equilibrium ($p > 0.001$), linkage disequilibrium (LD), and haplotype frequencies were calculated using the Haploview software (version 4.2) (26).

Protein and cytokine levels in ROP and control samples were represented as bar plot (the mean ± SE) and box plot (median, interquartile range, and whiskers). Comparison of proteins and cytokines levels between ROP and controls vitreous/tears were calculated using the unpaired Student's $t$-test. A $p$-value $< 0.05$ was considered to be statistically significant. Since the cytosolic calcium level does not follow a normal distribution, we performed the testing of equality in medians for control and hypoxic condition using Wilcoxon rank-sum test.

# RESULTS

## Involvement of Genes in ROP

Of the 384 variants screened (Table S2 in Supplementary Material), 73 were removed from further analysis as they were either not in Hardy-Weinberg equilibrium in the controls ($n = 16$), were monomorphic ($n = 44$), or had a call rate < 97% ($n = 13$). Thus, 311 SNPs from 26 genes were finally analyzed for association with ROP. Among these 37 SNPs in 14 genes (*AGTR1, ANGPT2, C3, CFH, CFB, CXCR4, FBLN5, H2AFX, IHH, MMP2, TGF*β*1, CETP, VEGF*, and *TSPAN12*) exhibited significant association ($p < 0.05$) with ROP (**Table 1**). Additionally, 5/37 associated SNPs in *CFH, CFB, CXCR4, FBLN5,* and *CETP* genes withstood Bonferroni correction. Intriguingly, only the *CETP* variant (rs891141) conferred significant risk of ROP, while the variants across the other genes were protective (**Table 1**). Strong LD was observed across all the variants (except rs1831821) in *CFH* and rs891141 and rs289716 in *CETP* gene, while moderate LD was observed between rs891141 and rs289713 in *CETP* and rs2268002 and rs2284340 in *FBLN5* (Figure S1 in Supplementary Material).

Likewise, haplotypes generated with the associated and flanking variants of these five genes revealed that only the haplotype C-A-T in *CETP* conferred significant risk of ROP, while those with *CFH* and *FBLN5* were protective. Haplotypes with the *CXCR4* and *CFB* were not informative (**Table 2**). Thus, the present study highlights the potential involvement of novel genes (*CFH, CFB, CETP, FBLN5,* and *CXCR4*) in ROP based on their allelic and haplotype associations.

## Quantitative Assessment of Proteins Involved in Complement Cascade and Neurodegeneration in the Vitreous Samples of ROP Subjects

Based on strong associations in the *CFH* and *CFB* genes, a quantitative assessment of a neurodegenerative panel containing CRP, SAP, MIP-4, Complement C4, apolipoprotein AI, apolipoprotein CIII, apolipoprotein E, Complement Factor H, and Complement C3 proteins was carried out by multiplex immuno-bead assay in the vitreous samples of ROP patients ($n = 30$) and controls ($n = 30$). All the complement components and apolipoproteins were detectable in the vitreous samples. Overall, we observed significantly elevated levels of C3 ($p = 0.05$), C4 ($p = 0.001$), CFH ($p = 2.24 \times 10^{-5}$), VEGF ($p = 0.0027$), apolipoprotein AI ($p = 0.0007$), and apolipoprotein CIII ($p = 0.004$) in the vitreous of ROP compared to the control subjects indicating their possible involvement in the disease pathogenesis (**Figure 1A**).

## Activation of Complement Pathway in Vitreous Humor of Proliferative ROP

We validated the differential expression of complement component C3 by western blotting. An intense band of 192 kDa corresponding to C3 molecule was observed in ROP cases compared to controls (**Figure 1B**). Additionally, we observed the activated C3 fragments; C3b (182 kDa), C3c (145 kDa), and iC3bα (63 kDa) in the ROP vitreous under non-reducing conditions as confirmed by mass spectrometry (data not shown here), but not in the controls (**Figure 1B**), suggesting a higher activation of C3 in ROP. Likewise, a higher expression of complement component C5 was observed in ROP vitreous compared to the controls (data not shown) suggesting a further activation of the complement pathway.

## Hypoxia-Induced Activated Macrophage Secretes Angiogenic Molecules

We further demonstrated that along with increased expression of angiogenic molecules in the vitreous samples of patients, activated macrophages/microglia in turn would also be secreting proinflammatory cytokines that might exacerbate the inflammation, further playing a role in the ROP pathogenesis. We detected activated macrophages/microglia on H&E, further confirmed by immunostaining with CD68 in ROP vitreous but not in the controls (**Figure 1C**). The results of this experiment supported for shift in the proangiogenic state as demonstrated by a significant increase in the levels of cytokines IL8 ($p = 0.0149$), G-CSF ($p = 0.0099$), IL1ra ($p = 0.0019$),

**TABLE 1** | Association of gene variants with retinopathy of prematurity (ROP).

| Genes screened | Single-nucleotide polymorphism (SNP) ID | Location | Nucleotide change | Amino acid change | RegulomeDB (binding score) (27) | Minor allele | Minor allele frequencies | | *p*-Value | Odds ratio [95% CI] |
|---|---|---|---|---|---|---|---|---|---|---|
| | | | | | | | ROP | Controls | | |
| *CFH* | **rs374896** | **Intron** | g.71371T>C | – | Minimum binding evidence (6) | **T** | **0.0426** | **0.159** | **$2.94 \times 10^{-7}$** | **0.241 [0.135–0.431]** |
| *CFB* | **rs1048709** | **Exon** | g.19461A>G | p.R150R | Likely to affect binding of POLR2A and linked expression of the HLAC, HLA-DQA1, HLADQB1, HLADRB1, HLADRB5 | **G** | **0.15** | **0.269** | **$1.71 \times 10^{-5}$** | **0.484 [0.035–0.676]** |
| *C3* | rs344550 | Intron | g.37710G>C | – | Likely to affect binding of GATA2, MYC, NR2F2, STAT5A, SPI1CCNT2 (1F) | C | 0.223 | 0.29 | 0.0409 | 0.703 [0.501–0.986] |
| | rs2287846 | Intron | g.24106G>C | – | Minimal binding evidence (5) | G | 0.298 | 0.237 | 0.0658 | 1.370 [0.979–1.915] |
| *CXCR4* | **rs2228014** | **Exon** | g.2652C>T | p.I142I | Minimum binding evidence (4) | **G** | **0.422** | **0.637** | **$1.32 \times 10^{-8}$** | **0.416 [0.307–0.565]** |
| *ANGPT2* | rs2922889 | Intron | g.119194A>T | – | Minimum binding evidence (6) | T | 0.497 | 0.431 | 0.0776 | 1.305 [0.971–1.756] |
| | rs2515464 | Intron | g.35092A>C | – | Minimum binding evidence (5) | T | 0.173 | 0.251 | 0.0102 | 0.622 [0.432–0.895] |
| | rs734701 | Intron | g.32684C>T | – | Minimum binding evidence (6) | A | 0.452 | 0.527 | 0.0465 | 0.741 [0.551–0.996] |
| | rs2959812 | Intron | g.29629T>C | – | Minimum binding evidence (5) | C | 0.471 | 0.548 | 0.0391 | 0.732 [0.544–0.985] |
| *VEGF* | rs2010963 | 5′-UTR | – | – | Minimum binding evidence (4) | C | 0.302 | 0.243 | 0.0084 | 1.352 [0.969–1.888] |
| | rs1413711 | Intron | g.2758T>C | – | Minimum binding evidence (4) | T | 0.39 | 0.482 | 0.014 | 0.688 [0.51–0.928] |
| | rs1005230 | Intergenic | – | – | Minimum binding evidence (5) | A | 0.388 | 0.482 | 0.011 | 0.680 [0.505–0.917] |
| *FBLN5* | **rs2268002** | **Intron** | g.17582G>C | – | Minimum binding evidence (5) | **G** | **0.32** | **0.423** | **$9.2 \times 10^{-4}$** | **0.641 [0.492–0.835]** |
| *MMP2* | rs2285052 | Intron | g.88546A>C | – | Minimum binding evidence (5) | G | 0.092 | 0.036 | 0.0025 | 2.732 [1.39–5.368] |
| *TGFb1* | rs11466359 | Intron | g.22217C>T | – | Minimum binding evidence (5) | T | 0.093 | 0.0482 | 0.021 | 2.027 [1.1–3.734] |
| | rs4803457 | Upstream | g.4544T>C | – | Minimum binding evidence (4) | A | 0.465 | 0.536 | 0.061 | 0.754 [0.561–1.013] |
| *CETP* | **rs891141** | **Intron** | g.7962G>T | – | Minimum binding evidence (5) | **C** | **0.234** | **0.114** | **$2.99 \times 10^{-5}$** | **2.378 [1.57–3.598]** |
| *H2AFX* | rs640603 | Intergenic 3′ of a gene | – | – | Likely to affect binding of PLR2A, CHD1, E2F6, MXI1, E2F4, E2F6, MYC (2b) | T | 0.161 | 0.09 | 0.0049 | 1.940 [1.215–3.085] |
| *TSPAN12* | rs41624 | Intron | g.62819A>G | – | Minimum binding evidence (6) | T | 0.176 | 0.243 | 0.0279 | 0.665 [0.462–0.958] |
| | rs41629 | Intron | g.59568T>G | – | Minimum binding evidence (6) | A | 0.176 | 0.243 | 0.0279 | 0.665 [0.462–0.958] |
| | rs3735467 | Intron | g.47721G>T | – | Minimum binding evidence (5) | C | 0.177 | 0.246 | 0.031 | 0.669 [0.465–0.964] |
| | rs12669167 | Intron | g.38926T>G | – | NA (7) | C | 0.173 | 0.24 | 0.0279 | 0.664 [0.46–0.958] |
| | rs10225453 | Intron | g.36511C>A | – | Minimum binding evidence (5) | T | 0.17 | 0.236 | 0.0287 | 0.663 [0.458–0.959] |
| | rs6953454 | Intron | g.33908G>A | – | NA (7) | T | 0.172 | 0.237 | 0.03 | 0.666 [0.461–0.964] |
| | rs996903 | Intron | g.32898A>G | – | Likely to affect binding and linked expression of the FLJ21986 (1F) | C | 0.17 | 0.237 | 0.0279 | 0.662 [0.458–1.044] |
| | rs6959328 | Intron | g.32490T>A | – | NA (7) | A | 0.17 | 0.237 | 0.0279 | 0.662 [0.458–1.044] |
| | rs6466759 | Intron | g.28767A>T | – | Minimum binding evidence (5) | T | 0.17 | 0.238 | 0.0251 | 0.657 [0.454–0.95] |
| | rs7805211 | Intron | g.25107G>A | – | Minimum binding evidence (6) | A | 0.168 | 0.237 | 0.0218 | 0.65 [0.449–0.941] |
| | rs6466760 | Intron | g.24403C>G | – | Minimum binding evidence (6) | C | 0.168 | 0.237 | 0.0218 | 0.65 [0.449–0.941] |
| | rs6466762 | Intron | g.16639G>A | – | Minimum binding evidence (5) | A | 0.169 | 0.241 | 0.0167 | 0.638 [0.441–0.923] |
| | rs3823859 | Intron | – | – | Minimum binding evidence (5) | G | 0.17 | 0.24 | 0.0219 | 0.651 [0.451–0.941] |
| | rs17142995 | Intron | g.11660A>G | – | Minimum binding evidence (6) | C | 0.173 | 0.24 | 0.0279 | 0.664 [0.46–0.958] |
| | rs7781985 | Intron | g.6475A>C | – | Likely to affect binding and linked expression of the FLJ21986/ monocytes (1F) | C | 0.17 | 0.24 | 0.0219 | 0.651 [0.451–0.941] |
| | rs3757557 | 5′UTR | g.91G>A | – | Minimum binding evidence (4) | A | 0.117 | 0.171 | 0.0411 | 0.644 [0.421–0.985] |
| | rs4141309 | Intergenic, upstream 5′ of gene | – | – | Minimum binding evidence (4) | A | 0.112 | 0.171 | 0.0236 | 0.611 [0.398–0.939] |
| *AGTR1* | rs2739504 | Intron | g.13100A>G | – | Minimum binding evidence (4) | C | 0.446 | 0.371 | 0.041 | 1.362 [1.012–1.833] |
| *IHH* | rs394452 | Exon | g.5153T>C | p.T376T | Minimum binding evidence (5) | T | 0.261 | 0.168 | 0.0027 | 1.75 [1.211–2.528] |

*SNPs in bold withstood Bonferroni correction.*

**TABLE 2** | Estimated haplotype frequencies of the significantly associated variants in *CETP, CFH*, and *FBLN5* genes in retinopathy of prematurity (ROP) and premature controls.

| Genes (single-nucleotide polymorphisms) | Haplotypes | Overall frequencies | ROP frequencies | Controls frequencies | Chi square | *p*-Value | Odds ratios (95% CI) |
|---|---|---|---|---|---|---|---|
| *CETP* (rs891141, rs289713, rs289716) | A-A-T | 0.327 | 0.313 | 0.343 | 0.734 | 0.3916 | 0.871 (0.637–1.193) |
| | A-A-A | 0.3 | 0.294 | 0.308 | 0.156 | 0.6931 | 0.937 (0.68–1.292) |
| | C-A-T | 0.149 | 0.191 | 0.101 | 11.358 | 0.0008 | 2.1 (1.354–3.256) |
| | A-T-A | 0.143 | 0.121 | 0.169 | 3.357 | 0.0669 | 0.674 (0.442–1.029) |
| | A-T-T | 0.053 | 0.04 | 0.067 | 2.488 | 0.1147 | 0.586 (0.3–1.144) |
| *CFH* (rs3753395, rs374896, rs393955) | T-C-T | 0.563 | 0.578 | 0.547 | 0.693 | 0.4052 | 1.134 (0.843–1.526) |
| | A-C-G | 0.188 | 0.233 | 0.139 | 10.066 | 0.0015 | 1.874 (1.268–2.769) |
| | A-C-T | 0.151 | 0.149 | 0.154 | 0.032 | 0.8586 | 0.962 (0.638–1.451) |
| | A-T-G | 0.096 | 0.04 | 0.156 | 27.61 | $1.48 \times 10^{-7}$ | 0.226 (0.125–0.41) |
| *FBLN5* (rs2268002, rs2284340) | G-C | 0.38 | 0.413 | 0.343 | 3.621 | 0.0571 | 1.346 (0.992–1.826) |
| | G-G | 0.37 | 0.311 | 0.437 | 12.093 | $5 \times 10^{-4}$ | 0.58 (0.427–0.789) |
| | A-C | 0.242 | 0.271 | 0.21 | 3.625 | 0.0569 | 1.4 (0.989–1.983) |

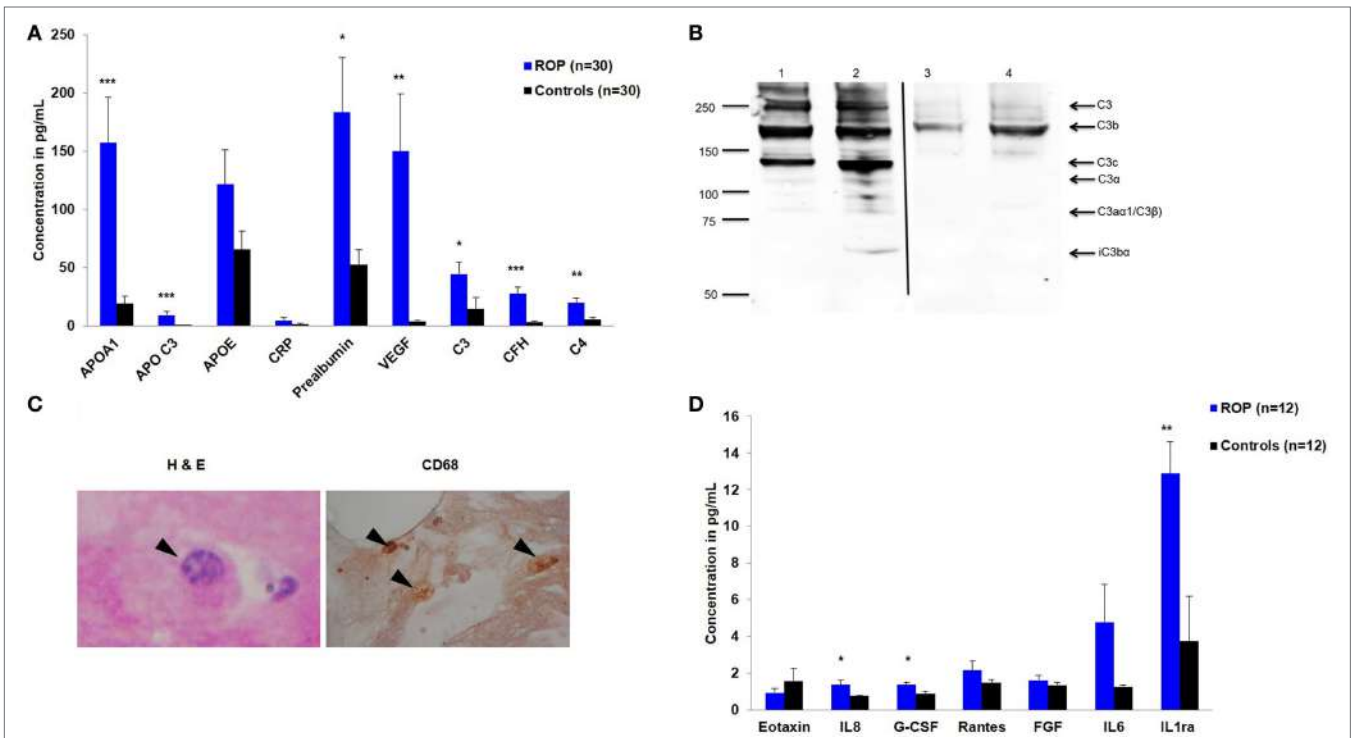


**FIGURE 1** | Expression of inflammatory molecules in proliferative retinopathy of prematurity (ROP). **(A)** Differential levels of complement components and apolipoproteins in the vitreous humor of ROP and controls **(B)** Western blotting of C3 done under non-reducing condition, showing its expression in patients (lane 1 and 2) and controls (lane 3 and 4). Arrows indicate the C3 fragments. Thin black line inserted within gel showing that all the lanes were run on the same gel but were not continuous **(C)** Hematoxylin and eosin staining of ROP vitreous. Arrowheads indicate degenerated morphology of macrophages at 40×-magnification (irregular shaped with large vacuole, nucleus with a very prominent nucleolus); Staining of ROP vitreous with CD68 marker. Arrowheads indicate the presence of activated macrophages at 10× magnification. **(D)** Differential levels of inflammatory cytokines in the vitreous humor of ROP and controls. Error bars in **(A)** and **(D)** show SEM, $^{*}p < 0.05$, $^{**}p < 0.005$, $^{***}p < 0.0005$ (ROP vs. controls).

and VEGF ($p = 0.0027$) (**Figures 1A,D**) along with marginal increase of IL6, IL12, IL7, RANTES, and MCP1 in the ROP vitreous (data not shown).

To further confirm these results, we subjected the cultured microglial cells to hypoxic condition and checked for the expression of proinflammatory markers. The effect of hypoxia on the activation of macrophages/microglia was observed with an intense calcium staining in cells exposed to hypoxia compared to the unexposed ones. The result shows that there is increase in cytosolic calcium levels in case of hyperactivated cells subjected to 24 h of hypoxic stress (**Figure 2A**, $n = 50$). Specifically, there is a significant increase ($p < 0.0005$) in cytosolic calcium

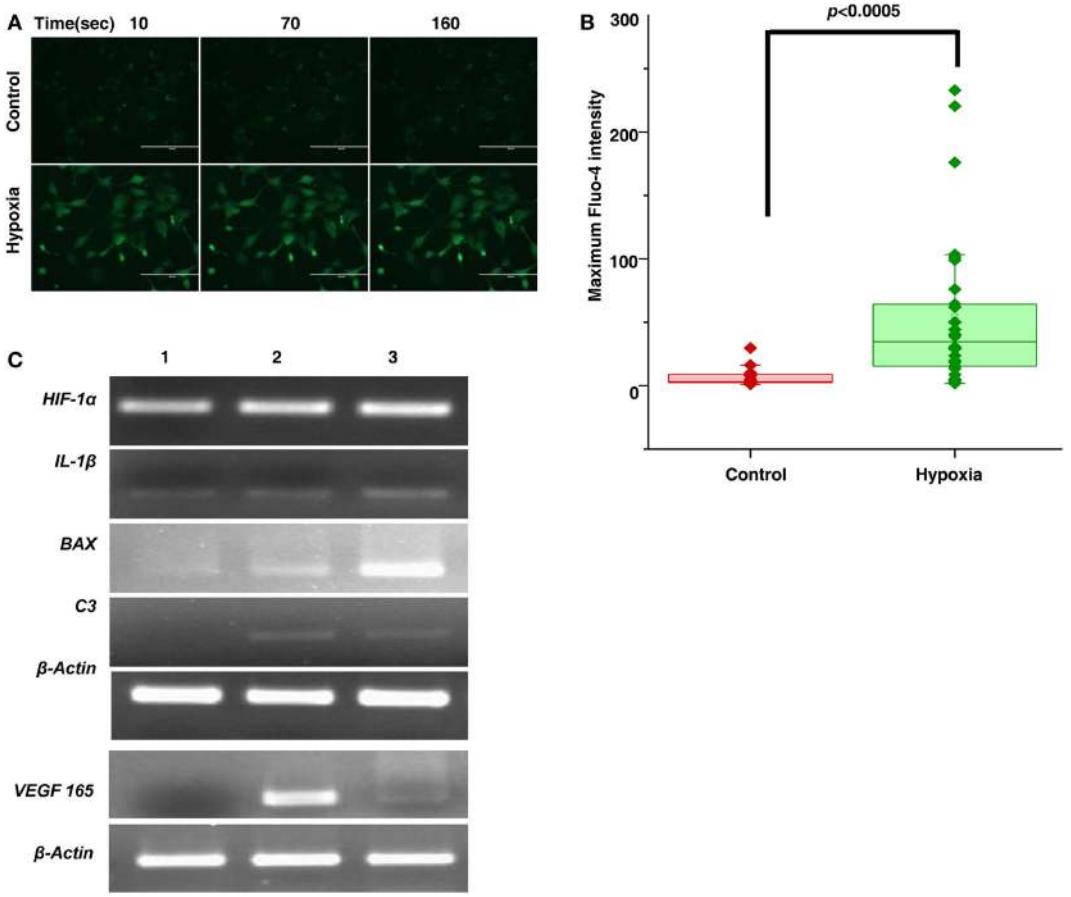


**FIGURE 2** | Hypoxia induced microglia secretes inflammatory and angiogenic molecules. **(A)** Time lapse imaging of cytosolic calcium in microglial cells in normal and hypoxic conditions. Scale bar: 200 μm **(B)** Comparison of $Ca_{max}$ (Maximum Fluo-4 intensity) in microglial cells for control and hypoxic condition [$Ca^{2+}$transients were measured for 50 cells ($n = 50$) for each cases]. Data are presented as box plot and were analyzed using Wilcoxon rank-sum test. **(C)** Semi-quantitative PCR was used to evaluate the expression of secreted product (*HIF-1α, IL-1β, BAX, C3, VEGF*) of hypoxia-induced microglial cells treated with no $CoCl_2$ (lane 1), 100 μM $CoCl_2$ (lane 2), and 150 μM $CoCl_2$ (lane 3) and β-actin as control.

($Ca_{max}$ = the maximum Fluo-4 intensity) in microglial cells followed by hypoxia exposure (**Figure 2B**). Likewise, a higher expression of complement *C3, VEGF165,* and hypoxia inducing factor-1α (*HIF-1α*) was also observed in exposed cells (**Figure 2C**).

## Involvement of Extra-Matrix Metalloproteinases in Pathogenesis of ROP

A strong association of SNPs in *FBLN5* and moderate association of *MMP2, TGF*β gene (**Table 1**) with ROP suggested the role of ECM proteins in ROP pathogenesis. Further, a quantitative assessment of the ECM proteins indicated a significant increase in MMP9 ($p = 0.038$), TIMP1 ($p = 0.004$), and α2 macroglobulin ($p = 0.0018$) in the ROP vitreous (**Figure 3A**). We also assessed the MMP activation in ROP by gelatine zymography. Our results showed higher levels of both pro and activated MMPs (MMP9 and/or MMP2) in the vitreous of patients suggesting its potential role in disease pathogenesis (**Figure 3B**).

## Exploring the Potential of Inflammatory Markers in Tear Samples for the Progression of ROP

We explored if increased expression of inflammatory markers (as seen in the vitreous samples of ROP patients) could also be reproducibly detected in tears and further be established as the biomarker for disease progression. A quick multiplex ELISA of tear samples collected from the ROP babies at different stages and no-ROP preterms was performed for some inflammatory markers (interleukins, TNFα, IFNγ, and MMPs). Significantly higher expressions of IL-1ra ($p = 0.014$), MMP2 ($p = 0.0085$), and MMP-9 ($p = 0.03$) were detected in severe ROP cases compared to mild ROP and no-ROP tear samples that was further confirmed by zymography (**Figures 3C–E**). On the zymogram, the tear samples from no-ROP showed very low expression of MMPs as compared to severe ROP (**Figure 3E**). These results were confirmed to be reproducible in the extended cohort of ROP with a significant increased expression of activated MMP2 in severe ROP ($p = 0.0023$) and progressive ROP ($p = 0.007$) as compared

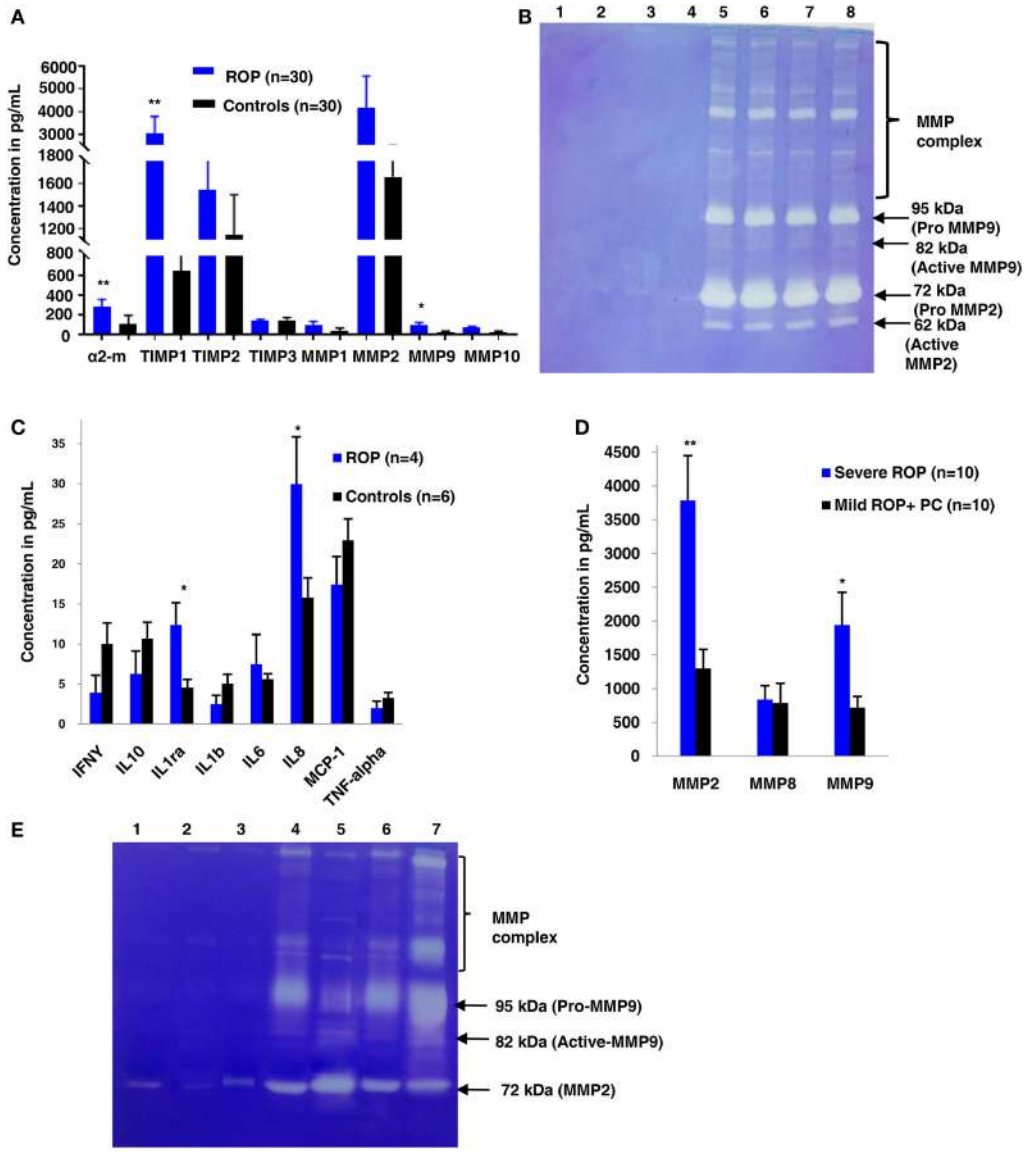


**FIGURE 3** | Extracellular matrix (ECM) metalloproteinases and cytokines increases in proliferative retinopathy of prematurity (ROP) in both vitreous and tears samples. **(A)** Differential levels of ECM proteins and its inhibitors in ROP and control vitreous [*$p < 0.05$, **$p < 0.005$, *** $p < 0.0005$ (ROP vs. controls)]. **(B)** Zymogram shows activation of MMPs in ROP vitreous (lanes 5, 6, 7, 8) as compared to controls (1, 2, 3, 4). **(C)** Differential levels of cytokines in ROP (5 μL) and control tears (5 μL). **(D)** Differential levels of MMPs in ROP (5 μL) and control tear (5 μL) [*$p < 0.05$, **$p < 0.005$, ***$p < 0.0005$ (severe ROP vs. mild ROP + premature controls)]. **(E)** Zymography showing more activation of MMPs in severe ROP (lanes 6, 7) as compared to mild ROP (lanes 4,5) and controls (5 μL tears; lanes 1, 2, 3). Error bars show SEM.

to mild ROP ($p = 0.01$) and premature controls. Similar pattern of gradual increase in MMP9 expression was also observed in mild ROP ($p = 0.02$) to progressive ($p = 0.001$) and severe ROP cases ($p = 1.2 \times 10^{-6}$) with respect to premature controls (**Figure 4**).

## DISCUSSION

Retinopathy of prematurity is a biphasic disease that includes an initial phase of hyperoxia leading to blood vessel obliteration followed by hypoxia causing vessel proliferation eventually leading to neovascularization and neurodegeneration. It is a complex disease with multifactorial etiologies. An earlier study on monozygotic and dizygotic twin pairs had also noted the genetic involvement in the development of ROP, in absence of other environmental factors (28). While supplemental oxygen is considered as a major risk factor along with lower GA and BW, studies from India and other Asian countries have reported ROP babies with higher GA and BW (29) and oxygen supplementation does not always predict the risk of ROP (6). Therefore, we hypothesized that genetic predisposition along with environmental/maternal or other risk factors may lead to the development of ROP.

A strong association of gene variants involved in the complement pathway (*CFH, CFB, C3*), ECM remodeling (*FBLN5*, *MMP9*), leukocyte transendothelial migration and activation

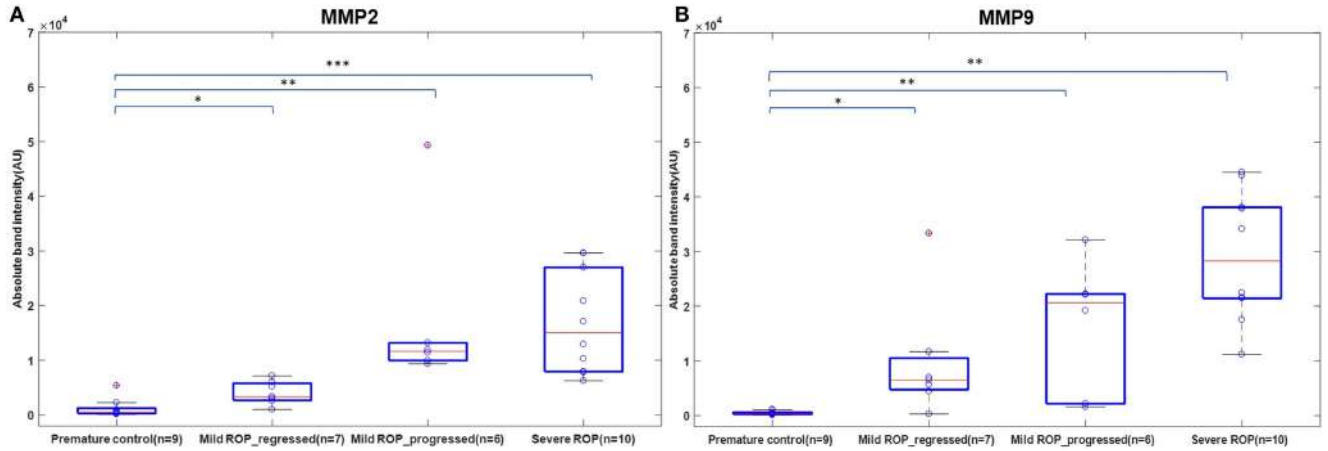


**FIGURE 4** | A role of MMPs in tears as biomarker for retinopathy of prematurity (ROP) progression: differential expression of Zymogram band intensities of **(A)** MMP9 and **(B)** MMP2 in extended cohort including severe ROP ($n$ = 10), mild ROP_progressed ($n$ = 6), mild ROP_regressed ($n$ = 7), and no ROP premature controls ($n$ = 9) [*$p$ < 0.05, **$p$ < 0.005, *** $p$ < 0.0005 (ROP vs. controls)], AU, arbitrary unit.

(*CXCR4*), HIF1A signaling and angiogenesis (*ANGPT2, H2AFX,* and *VEGF*), and developmental processes (*TGFb1, IHH*) observed in the present study (**Table 1**), confirms the involvement of genes in ROP pathogenesis. A previous study reported the association of polymorphisms in *IHH, AGTR1, TBX5, CETP, GP1BA, EPAS1, BDNF,* and *CFH* with ROP (11, 13). However, only a few of these associated variants could be replicated in the present cohort, indicating allelic heterogeneity (**Table 3**). Thus, the novel and associated variants identified in the present study (**Tables 1** and **3**) and elsewhere should be screened across multiple populations to understand their implications in ROP.

The strong associations of *CFH*, *CFB*, and *C3* variants in our ROP patients along with elevated levels of C3 and CFH proteins in their vitreous (**Table 1** and **Figure 1A**) indicated a possible involvement of the alternative complement pathway in ROP. CFH and CFB are the regulators of the alternative complement immune pathway (30). Upon activation, CFB is cleaved by complement factor D yielding two subunits, Ba and Bb. The active subunit Bb associates with C3b to form C3 convertase of alternative pathway while CFH regulates the alternative pathway activation by accelerating the decay of C3 convertase (30). It was also noted that there was an increase in the formation of CFB in oxygen induced retinopathy (OIR) mice model (31). Thus, the observed genetic associations of *CFH* and *CFB* complemented with their increased expression of cleaved C3 protein fragments in the vitreous of ROP-affected eyes in our study confirmed their possible involvement in disease pathogenesis (**Figure 5**). Generally, complement factors are known to be downregulated in the normal preterm neonates because of immature development of the immune system (32, 33). On the contrary, we observed an elevation and activation of the complement components and complement factors in the vitreous of ROP patients at infancy (**Figure 1**), suggesting an important role of the complement pathway in ROP pathogenesis.

Interestingly, the genetic variants in *CFH, C3,* and *CFB* genes have also been associated with AMD susceptibility (34, 35).

**TABLE 3** | Comparison of commonly associated gene variants in retinopathy of prematurity worldwide.

| Associated genes | Associated single-nucleotide polymorphisms (associated allele) | Present study (India), [a]189/167 | Study by Mohamed et al. (11) (U.K.), [a]102/228 | Study by Hartnett et al. (13) (USA), [a]593/364 |
|---|---|---|---|---|
| *CFH* | rs529825 (A) | $p$ = 0.7521 | $p$ = 0.01 | – |
| | rs800292 (A) | $p$ = 0.3186 | $p$ = 0.01 | – |
| | rs379489 (A) | $p$ = 0.4343 | – | $p$ = 0.3926 |
| | rs395544 (A) | $p$ = 0.5525 | – | $p$ = 0.403 |
| *CETP* | rs289747 (T) | $p$ = 0.5688 | $p$ = 0.004 | – |
| *GP1BA* | rs2243093 (C) | $p$ = 0.2991 | $p$ = 0.005 | – |
| *TBX5* | rs1895602 (T) | $p$ = 0.352 | $p$ = 0.003 | – |
| *AGTR1* | rs33978228 (G) | $p$ = 0.0196 | – | – |
| | rs427832 (G) | $p$ = 0.2177 | $p$ = 0.005 | – |
| *IHH* | rs3099 (C) | $p$ = 0.1565 | $p$ = 0.003 | – |
| *EPAS1* | rs1867785 (G) | $p$ = 0.958 | $p$ = 0.001 | – |

[a]*Cases/controls.*

A Y402H variant in the *CFH* gene was found to be most strongly associated with AMD patients worldwide. However, the ROP-associated *CFH* variant (rs374896) identified in the present study is located in the intron of the gene (**Table 1**). Further, functional studies on CFH in AMD eyes have shown that chronic low grade intraocular complement activation in patients carrying the risk variants in *CFH* along with exposure to environmental triggers (smoking, oxidative stress, etc.) causes the retinal pigment epithelial damage leading to neurodegeneration and neovascularization and eventually visual loss (36).

Complement components do not mediate neovascularization by itself but *via* the inflammatory cells (37). As was demonstrated in an OIR mouse model, complement factors C3a and C5a activate macrophages by binding to C3aR and C5aR, thereby regulating angiogenesis (38). In the present study, a strong association ($p = 1.32 \times 10^{-8}$) of rs2228014 in *CXCR4* (**Table 1**) along with the presence of activated microglia/macrophages in the vitreous

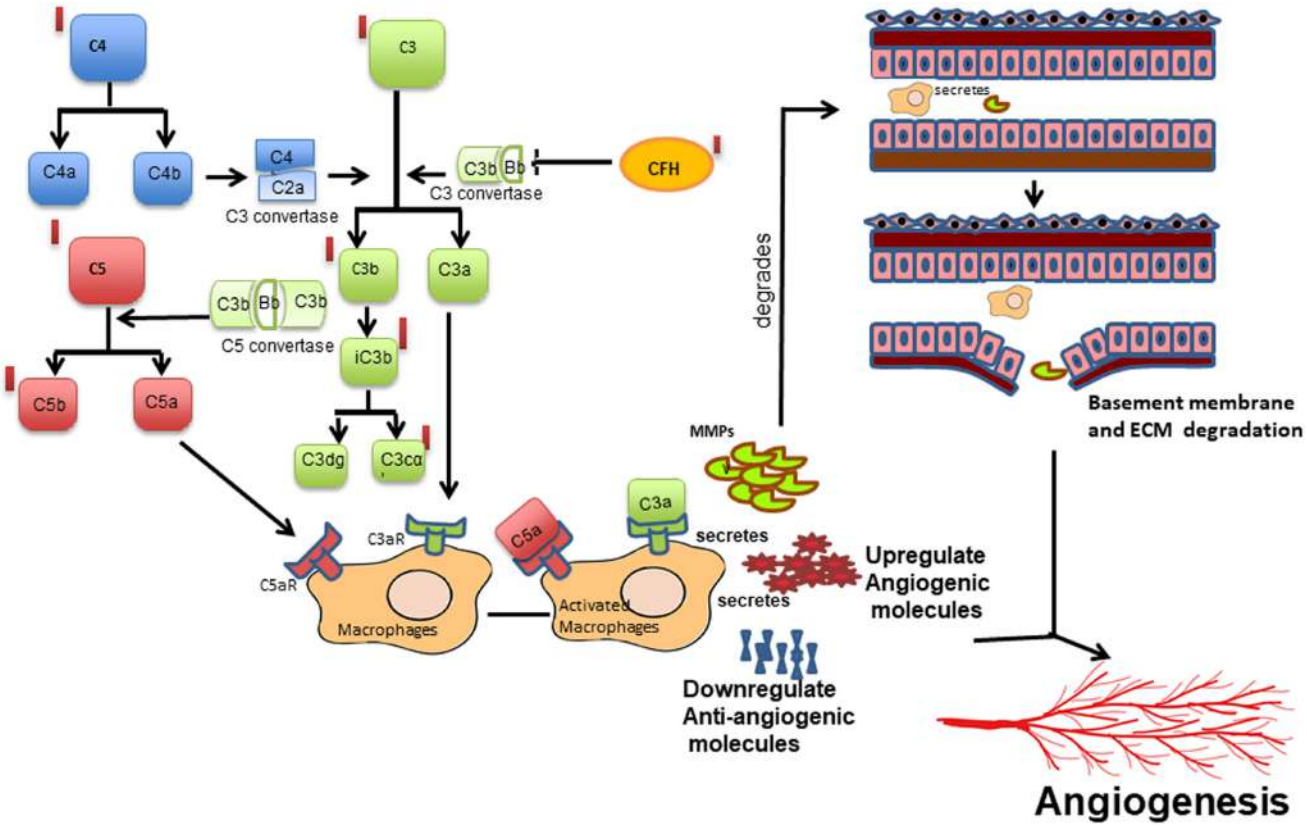


**FIGURE 5** | Schematic diagram of the proposed mechanism of complement activation and its potential effect on macrophage-mediated angiogenesis in retinopathy of prematurity. Cleavage of complement components C3 into C3a, C3b and further into iC3b, C3dg and C3cα; C4 into C4a and C4b and C5 into C5a and C5b leading to the activation of complement cascade, which in turn activates macrophage/microglia or *vice versa*. Activated macrophage/microglia secretes MMPs, cytokines, proangiogenic proteins, and reduced angiogenesis inhibitors that may lead to increased vessel proliferation and extracellular matrix (ECM) degradation in turn promoting angiogenesis. Red bars represent upregulation of the complement components observed in the present study.

(**Figure 1C**), implicate their role in ROP angiogenesis via the leukocyte transendothelial migration. CXCR4 is a chemokine receptor for stromal derived factor 1 (CXCL12/SDF-1), which is mainly involved in the extravasation and migration of lymphocytes and monocytes (39). Inhibition of CXCR4 has been shown to result in reduced vascular sprouting following VEGF treatment in retinal explants (40). Our observation of the association of variants in *VEGF, ANGPT2,* and *H2AFX* (**Table 1**) indicate the involvement of HIF1α signaling pathway (hypoxia) in ROP pathogenesis. Furthermore, the secretion of C3 and VEGF by microglial cells under hypoxia (**Figure 2**) validated that hypoxia induced microglia/macrophage along with the complement component, could be contributing to the neovascularization in ROP eyes. The high level of α2-macroglobulin in the ROP vitreous (**Figure 3A**) also indicated the presence of activated macrophages/microglia that further interacts with low-density lipoprotein receptor-related protein 1 (LRP1) which in turn induces MMP9 expression (41, 42).

Based on published studies on macrophages/microglia activation leading to inflammation (37), we proposed that increased expression of the complement components, VEGF, other cytokines, and ECM components (MMPs) in the vitreous of ROP patients are mediated by macrophage/microglia activation by creating an imbalance of angiogenic and anti-angiogenic molecules (**Figure 5**). The proteolytic degradation of ECM is a critical step for the invasion of blood vessels during neovascularization. MMPs are endoproteases that cleaves the protein components of the ECM while TIMPs, α2 macroglobulins, and α1 antitrypsin are the proteinase inhibitors (43). In proliferative diabetic retinopathy, the elevated levels of MMP-2 and MMP-9 were shown to cause ECM remodeling (44, 45) further leading to net collagen IV degradation and vitreous liquefaction (46). The presence of activated MMP-9 in the vitreous along with elevated levels of TIMP1, TIMP2, and α2 macroglobulin in our ROP patients and presence of blood component proteins like apolipoproteins (**Figures 1A** and **3A**) explained its role in the degradation of the basement membrane of blood vessels, seeping out into the vitreous along with the other blood components, thereby causing vitreous hemorrhage and vitreous liquefaction.

Presence of inflammatory markers in the vitreous or other body fluid in young preterm babies might suggest an infectious etiology and inflammatory stimuli contributing to ROP (47). Fetal inflammatory response syndrome (including sepsis, periventricular leukomalacia, intraventricular hemorrhage, necrotizing enterocolitis, and bronchopulmonary dysplasia), chorioamnionitis, and microbial infections are some of the predisposing factors for

inflammation observed in some studies (48). There was no evidence of exposure to infection in our cohort since babies with any microbial infections were excluded. Additionally, we did not find any difference in the complement levels or activation patterns in the serum of these patients and controls unlike in the vitreous samples, further ruling out any systemic infection (data not shown). Based on these evidences, neonatal non-infectious inflammation might be playing a major role in the pathogenesis of ROP.

Based on these findings supplemented with increasing evidences on the role of inflammation in causing neovascularization, we speculated if MMPs could be detected in the tear samples of ROP babies so that it could be used as markers for ROP progression. The tear samples were an obvious choice for this study as it is fairly non-invasive, safe, and convenient, although there were some restrictions of tear volume and sampling in the ROP babies. It was interesting to note that the levels of MMPs in tears were significantly higher in severe ROP compared to no-ROP and mild ROP eyes that underscored its potential use as a biomarker for an early prediction of this condition (**Figures 3E** and **4**). This was further confirmed by zymography, with an increasing trend of the activated MMPs (both 2 and 9) in all the samples of severe stages of ROP along with a case of mild ROP. This mild ROP baby eventually progressed very quickly to a severe stage (plus ROP) in 2 weeks and did not respond to laser therapy (**Figure 3E**). The subsequent validation of these initial findings was done in an extended cohort and the increased levels of MMPs with the increase in severity of disease further established the usefulness of MMPs in tears as potential biomarkers. While our data proved that the levels of MMPs could reliably predict the progression of ROP (**Figure 4**), we could not perform any longitudinal analysis of MMPs levels in the tears due to the difficulties in obtaining samples from preterm babies at regular intervals. Likewise, a direct correlation of genotypes with protein levels or their activities in the corresponding biological material (vitreous/aqueous/tear) and clinical phenotype could not be attempted. Nevertheless, our study provided a proof of concept that tear MMPs levels could be a potential predictor for ROP progression in preterm babies.

In conclusion, the assessment of the activation of alternate complement pathway in ROP based on the novel genetic associations indicated the possible mechanisms of immune activation that could lead to aberrant neovascularization in the retina. However, the detailed underlying mechanisms of immune activation in abnormal blood vessel proliferation and neurodegeneration in the early stages of ROP are yet to be understood. Additionally, our results emphasized the primary role of complement component C3 in abnormal angiogenesis as seen in proliferative ROP. The proteins involved in the alternative complement pathway could be targeted selectively to prevent neovascularization, which might be helpful in preventing vision loss due the progression of ROP. The association of ECM-related genes with ROP along with elevated levels of the corresponding ECM proteins and its activation in the vitreous of ROP patients suggested its possible role in blood-retinal barrier degradation, which could promote neovascularization. Finally, the elevated levels of MMPs in tears of ROP patients established its role as a potential biomarker for the prediction of progression to proliferative stages. However, this needs to be replicated in other extended cohorts worldwide using a longitudinal study design. The present treatment strategies for managing severe ROP are inefficient as they target only the later vasoproliferative phase of ROP. Diagnosing and treating the disease at an earlier stage would definitely help in the timely and efficient management of this disease. The results of this study would aid in finding biomarkers for predictive testing as well as identifying newer drug targets for an efficient management of ROP.

## ETHICS STATEMENT

The study protocol adhered to the tenets of declaration of Helsinki and written informed consent was obtained from the parents of all the minor subjects and was approved by the Institutional Review Board (LEC02-14-029) of the L V Prasad Eye Institute (LVPEI).

## AUTHOR CONTRIBUTIONS

IK and SJ conceived the idea; IK, SJ, and SC wrote the protocol; IK served as principal investigator; SC, SJ, DB, RK, LG, PR, and PC were co-investigators; SJ, DB, RK, PR, and PC performed clinical examinations, graded the fundus images and did surgeries for the preterm and full term babies; SR, SP, and GM collected blood, vitreous and documented family history in the predesigned questionnaires; SR performed most of the molecular biology based analysis of blood and vitreous; SP performed the tear analysis; SSh performed cell biology work; LG and SS performed analysis for the $Ca^{2+}$ imaging data; SR, IK, and SC analyzed the data and wrote the manuscript; and all authors revised the paper and approved the submitted version.

## ACKNOWLEDGMENTS

The authors thank the parents of all the preterm and full term babies for their voluntary participation. The authors also thank Dr. Kumar Somasundaram (Indian Institute of Science, Bengaluru, India) for providing the human microglial cell line (CHME3) and Drs. Ch. Mohan Rao and T. Ramakrishna (Centre for Cellular and Molecular Biology, Hyderabad, India) for helping with a validation experiment using mass spectrometry.

## FUNDING

This work was supported by Department of Biotechnology (BT/01/COE/06/02/10 and BT/PR3992/MED/97/31/2011) Govt. of India; Champaulimaud Foundation, Portugal, and Hyderabad Eye Research Foundation. SR and SP were supported through fellowships of the Indian Council of Medical Research (ICMR) and the University Grants Commission (UGC) of the Government of India, respectively.

## SUPPLEMENTARY MATERIAL

The Supplementary Material for this article can be found online at http://www.frontiersin.org/articles/10.3389/fimmu.2017.01868/full#supplementary-material.

## REFERENCES


1. Gogate P, Gilbert C, Zin A. Severe visual impairment and blindness in infants: causes and opportunities for control. *Middle East Afr J Ophthalmol* (2011) 18:109–14. doi:10.4103/0974-9233.80698
2. Ludwig CA, Chen TA, Hernandez-Boussard T, Moshfeghi AA, Moshfeghi DM. The epidemiology of retinopathy of prematurity in the United States. *Ophthalmic Surg Lasers Imaging Retina* (2017) 48:553–62. doi:10.3928/23258160-20170630-06
3. Gergely K, Gerinec A. Retinopathy of prematurity – epidemics, incidence, prevalence, blindness. *Bratisl Lek Listy* (2010) 111:514–7.
4. Pejaver RK, Bilagi A, Vinekar A. *National Neonatology Foundation's Evidence Based Clinical Practice Guidelines for Retinopathy of Prematurity*. India: NNF (2010). p. 253–62.
5. Jalali S, Anand R, Kumar H, Dogra MR, Azad R, Gopal L. Programme planning and screening strategy in retinopathy of prematurity. *Indian J Ophthalmol* (2003) 51:89–99.
6. Chattopadhyay MP, Pradhan A, Singh R, Datta S. Incidence and risk factors for retinopathy of prematurity in neonates. *Indian Pediatr* (2015) 52:157–8. doi:10.1007/s13312-015-0594-1
7. Kumar P, Sankar MJ, Deorari A, Azad R, Chandra P, Agarwal R, et al. Risk factors for severe retinopathy of prematurity in preterm low birth weight neonates. *Indian J Pediatr* (2011) 78:812–6. doi:10.1007/s12098-011-0363-7
8. Csak K, Szabo V, Szabo A, Vannay A. Pathogenesis and genetic basis for retinopathy of prematurity. *Front Biosci* (2006) 11:908–20. doi:10.2741/1847
9. Krock BL, Skuli N, Simon MC. Hypoxia-induced angiogenesis: good and evil. *Genes Cancer* (2011) 2:1117–33. doi:10.1177/1947601911423654
10. Wang H, Zhang SX, Hartnett ME. Signaling pathways triggered by oxidative stress that mediate features of severe retinopathy of prematurity. *JAMA Ophthalmol* (2013) 131:80–5. doi:10.1001/jamaophthalmol.2013.986
11. Mohamed S, Schaa K, Cooper ME, Ahrens E, Alvarado A, Colaizy T, et al. Genetic contributions to the development of retinopathy of prematurity. *Pediatr Res* (2009) 65:193–7. doi:10.1203/PDR.0b013e31818d1dbd
12. Kondo H, Kusaka S, Yoshinaga A, Uchio E, Tawara A, Tahira T. Genetic variants of FZD4 and LRP5 genes in patients with advanced retinopathy of prematurity. *Mol Vis* (2013) 19:476–85.
13. Hartnett ME, Morrison MA, Smith S, Yanovitch TL, Young TL, Colaizy T, et al. Genetic variants associated with severe retinopathy of prematurity in extremely low birth weight infants. *Invest Ophthalmol Vis Sci* (2014) 55:6194–203. doi:10.1167/iovs.14-14841
14. Sato T, Kusaka S, Shimojo H, Fujikado T. Simultaneous analyses of vitreous levels of 27 cytokines in eyes with retinopathy of prematurity. *Ophthalmology* (2009) 116:2165–9. doi:10.1016/j.ophtha.2009.04.026
15. Sato T, Kusaka S, Shimojo H, Fujikado T. Vitreous levels of erythropoietin and vascular endothelial growth factor in eyes with retinopathy of prematurity. *Ophthalmology* (2009) 116:1599–603. doi:10.1016/j.ophtha.2008.12.023
16. Velez-Montoya R, Clapp C, Rivera JC, Garcia-Aguirre G, Morales-Canton V, Fromow-Guerra J, et al. Intraocular and systemic levels of vascular endothelial growth factor in advanced cases of retinopathy of prematurity. *Clin Ophthalmol* (2010) 4:947–53. doi:10.2147/OPTH.S11650
17. Yu H, Yuan L, Zou Y, Peng L, Wang Y, Li T, et al. Serum concentrations of cytokines in infants with retinopathy of prematurity. *APMIS* (2014) 122:818–23. doi:10.1111/apm.12223
18. Perez-Munuzuri A, Fernandez-Lorenzo JR, Couce-Pico ML, Blanco-Teijeiro MJ, Fraga-Bermudez JM. Serum levels of IGF1 are a useful predictor of retinopathy of prematurity. *Acta Paediatr* (2010) 99:519–25. doi:10.1111/j.1651-2227.2009.01677.x
19. Yenice O, Cerman E, Ashour A, Firat R, Haklar G, Sirikci O, et al. Serum erythropoietin, insulin-like growth factor 1, and vascular endothelial growth factor in etiopathogenesis of retinopathy of prematurity. *Ophthalmic Surg Lasers Imaging Retina* (2013) 44:549–54. doi:10.3928/23258160-20131105-05
20. Rathi S, Jalali S, Musada GR, Patnaik S, Balakrishnan D, Hussain A, et al. Mutation spectrum of NDP, FZD4 and TSPAN12 genes in Indian patients with retinopathy of prematurity. *Br J Ophthalmol* (2017). doi:10.1136/bjophthalmol-2017-310958
21. International Committee for the Classification of Retinopathy of Prematurity. The international classification of retinopathy of prematurity revisited. *Arch Ophthalmol* (2005) 123:991–9. doi:10.1001/archopht.123.7.991
22. Toth M, Fridman R. Assessment of gelatinases (MMP-2 and MMP-9) by gelatin zymography. *Methods Mol Med* (2001) 57:163–74. doi:10.1385/1-59259-136-1:163
23. Fischer AH, Jacobson KA, Rose J, Zeller R. Hematoxylin and eosin staining of tissue and cell sections. *CSH Protoc* (2008) 3:1–2. doi:10.1101/pdb.prot4986
24. Gupta RK, Swain S, Kankanamge D, Priyanka PD, Singh R, Mitra K, et al. Comparison of calcium dynamics and specific features for G protein-coupled receptor-targeting drugs using live cell imaging and automated analysis. *SLAS Discov* (2017) 22:848–58. doi:10.1177/2472555217693378
25. Rio DC, Ares M Jr, Hannon GJ, Nilsen TW. Purification of RNA using TRIzol (TRI reagent). *Cold Spring Harb Protoc* (2010) 2010:1–3. doi:10.1101/pdb.prot5439
26. Barrett JC, Fry B, Maller J, Daly MJ. Haploview: analysis and visualization of LD and haplotype maps. *Bioinformatics* (2005) 21:263–5. doi:10.1093/bioinformatics/bth457
27. Boyle AP, Hong EL, Hariharan M, Cheng Y, Schaub MA, Kasowski M, et al. Annotation of functional variation in personal genomes using RegulomeDB. *Genome Res* (2012) 22(9):1790–7. doi:10.1101/gr.137323.112
28. Bizzarro MJ, Hussain N, Jonsson B, Feng R, Ment LR, Gruen JR, et al. Genetic susceptibility to retinopathy of prematurity. *Pediatrics* (2006) 118:1858–63. doi:10.1542/peds.2006-1088
29. Jalali S, Matalia J, Hussain A, Anand R. Modification of screening criteria for retinopathy of prematurity in India and other middle-income countries. *Am J Ophthalmol* (2006) 141:966–8. doi:10.1016/j.ajo.2005.12.016
30. Noris M, Remuzzi G. Overview of complement activation and regulation. *Semin Nephrol* (2013) 33:479–92. doi:10.1016/j.semnephrol.2013.08.001
31. Sweigard JH, Yanai R, Gaissert P, Saint-Geniez M, Kataoka K, Thanos A, et al. The alternative complement pathway regulates pathological angiogenesis in the retina. *FASEB J* (2014) 28:3171–82. doi:10.1096/fj.14-251041
32. Wolach B, Dolfin T, Regev R, Gilboa S, Schlesinger M. The development of the complement system after 28 weeks' gestation. *Acta Paediatr* (1997) 86:523–7. doi:10.1111/j.1651-2227.1997.tb08924.x
33. Grumach AS, Ceccon ME, Rutz R, Fertig A, Kirschfink M. Complement profile in neonates of different gestational ages. *Scand J Immunol* (2014) 79:276–81. doi:10.1111/sji.12154
34. Klein RJ, Zeiss C, Chew EY, Tsai JY, Sackler RS, Haynes C, et al. Complement factor H polymorphism in age-related macular degeneration. *Science* (2005) 308:385–9. doi:10.1126/science.1109557
35. Francis PJ, Hamon SC, Ott J, Weleber RG, Klein ML. Polymorphisms in C2, CFB and C3 are associated with progression to advanced age related macular degeneration associated with visual loss. *J Med Genet* (2009) 46:300–7. doi:10.1136/jmg.2008.062737
36. Xu H, Chen M. Targeting the complement system for the management of retinal inflammatory and degenerative diseases. *Eur J Pharmacol* (2016) 787:94–104. doi:10.1016/j.ejphar.2016.03.001
37. Rutar M, Valter K, Natoli R, Provis JM. Synthesis and propagation of complement C3 by microglia/monocytes in the aging retina. *PLoS One* (2014) 9:e93343. doi:10.1371/journal.pone.0093343
38. Langer HF, Chung KJ, Orlova VV, Choi EY, Kaul S, Kruhlak MJ, et al. Complement-mediated inhibition of neovascularization reveals a point of convergence between innate immunity and angiogenesis. *Blood* (2010) 116:4395–403. doi:10.1182/blood-2010-01-261503
39. Bleul CC, Farzan M, Choe H, Parolin C, Clark-Lewis I, Sodroski J, et al. The lymphocyte chemoattractant SDF-1 is a ligand for LESTR/fusin and blocks HIV-1 entry. *Nature* (1996) 382:829–33. doi:10.1038/382829a0
40. Unoki N, Murakami T, Nishijima K, Ogino K, Van Rooijen N, Yoshimura N. SDF-1/CXCR4 contributes to the activation of tip cells and microglia in retinal angiogenesis. *Invest Ophthalmol Vis Sci* (2010) 51:3362–71. doi:10.1167/iovs.09-4978
41. Sanchez MC, Barcelona PF, Luna JD, Ortiz SG, Juarez PC, Riera CM, et al. Low-density lipoprotein receptor-related protein-1 (LRP-1) expression in a rat model of oxygen-induced retinal neovascularization. *Exp Eye Res* (2006) 83:1378–85. doi:10.1016/j.exer.2006.07.016
42. Caceres LC, Bonacci GR, Sanchez MC, Chiabrando GA. Activated alpha(2) macroglobulin induces matrix metalloproteinase 9 expression by low-density lipoprotein receptor-related protein 1 through MAPK-ERK1/2 and NF-kappaB activation in macrophage-derived cell lines. *J Cell Biochem* (2010) 111:607–17. doi:10.1002/jcb.22737

43. Visse R, Nagase H. Matrix metalloproteinases and tissue inhibitors of metalloproteinases: structure, function, and biochemistry. *Circ Res* (2003) 92:827–39. doi:10.1161/01.RES.0000070112.80711.3D
44. Noda K, Ishida S, Inoue M, Obata K, Oguchi Y, Okada Y, et al. Production and activation of matrix metalloproteinase-2 in proliferative diabetic retinopathy. *Invest Ophthalmol Vis Sci* (2003) 44:2163–70. doi:10.1167/iovs.02-0662
45. Descamps FJ, Martens E, Kangave D, Struyf S, Geboes K, Van Damme J, et al. The activated form of gelatinase B/matrix metalloproteinase-9 is associated with diabetic vitreous hemorrhage. *Exp Eye Res* (2006) 83:401–7. doi:10.1016/j.exer.2006.01.017
46. Coral K, Angayarkanni N, Madhavan J, Bharathselvi M, Ramakrishnan S, Nandi K, et al. Lysyl oxidase activity in the ocular tissues and the role of LOX in proliferative diabetic retinopathy and rhegmatogenous retinal detachment. *Invest Ophthalmol Vis Sci* (2008) 49:4746–52. doi:10.1167/iovs.07-1550
47. Dammann O. Inflammation and retinopathy of prematurity. *Acta Paediatr* (2010) 99:975–7. doi:10.1111/j.1651-2227.2010.01836.x
48. Sood BG, Madan A, Saha S, Schendel D, Thorsen P, Skogstrand K, et al. Perinatal systemic inflammatory response syndrome and retinopathy of prematurity. *Pediatr Res* (2010) 67:394–400. doi:10.1203/PDR.0b013e3181d01a36

**Conflict of Interest Statement:** The authors declare that the research was conducted in the absence of any commercial or financial relationships that could be construed as a potential conflict of interest.

Received: 5 January 2024 | Revised: 14 July 2024 | Accepted: 15 July 2024

DOI: 10.1111/jnc.16190

Journal of Neurochemistry JNC The Official Journal of the International Society for Neurochemistry WILEY

ORIGINAL ARTICLE

# Arachidonic acid metabolism regulates the development of retinopathy of prematurity among preterm infants

Saurabh Kumar[1,2] | Satish Patnaik[1] | Manjunath B. Joshi[3] | Neha Sharma[1,2] | Tarandeep Kaur[1] | Subhadra Jalali[4] | Ramesh Kekunnaya[5] | Aatish Mahajan[1] | Subhabrata Chakrabarti[1] | Inderjeet Kaur[1]

[1]Brien Holden Eye Research Centre, LV Prasad Eye Institute, Hyderabad, India

[2]Manipal Academy of Higher Education, Manipal, India

[3]Department of Ageing Research, Manipal School of Life Sciences, Manipal Academy of Higher Education, Manipal, India

[4]Smt. Kannuri Santhamma Centre for Vitreo Retinal Diseases, LV Prasad Eye Institute, Hyderabad, India

[5]Jasti V Ramanamma Children's Eye Care Centre, LV Prasad Eye Institute, Hyderabad, India

**Correspondence**
Inderjeet Kaur, Brien Holden Eye Research Centre, LV Prasad Eye Institute, Hyderabad, India.
Email: inderjeet@lvpei.org

**Present address**
Satish Patnaik, Brain Research Institute, University of California Los Angeles, Los Angeles, California, USA

Tarandeep Kaur, Department of Ophthalmology, Harvard Medical School, Boston, Massachusetts, USA

**Funding information**
Department of Biotechnology, Ministry of Science and Technology, India, Grant/Award Number: BT/PR32404/MED/30/2136/2019 and DBT/2020/LVPEI/1365; Wellcome Trust DBT India Alliance, Grant/Award Number: IA/E/22/1/506766; Impacting Research Innovation and Technology, Grant/Award Number: IMP/2018/001414; Department

## Abstract

Extremely preterm infants are at risk of developing retinopathy of prematurity (ROP), characterized by neovascularization and neuroinflammation leading to blindness. Polyunsaturated fatty acid (PUFA) supplementation is recommended in preterm infants to lower the risk of ROP, however, with no significant improvement in visual acuity. Reasonably, this could be as a result of the non-consideration of PUFA metabolizing enzymes. We hypothesize that abnormal metabolism of the arachidonic acid (AA) pathway may contribute to severe stages of ROP. The present study investigated the AA-metabolizing enzymes in ROP pathogenesis by a targeted gene expression analysis of blood (severe ROP = 70, No/Mild = 56), placenta (preterm placenta = 6, full term placenta = 3), and human primary retinal cell cultures and further confirmed at the protein level by performing IHC in sections of ROP retina. The lipid metabolites were identified by LC–MS in the vitreous humor (VH; severe ROP = 15, control = 15). Prostaglandins D2 ($p = 0.02$), leukotrienes B5 ($p = 0.0001$), 11,12-epoxyeicosatrienoic acid ($p = 0.01$), and lipid-metabolizing enzymes of the AA pathway such as *CYP1B1*, *CYP2C8*, *COX2*, and *ALOX15* were significantly upregulated while *EPHX2* was significantly (0.04) downregulated in ROP cases. Genes involved in hypoxic stress, angiogenesis, and apoptosis showed increased expression in ROP. An increase in the metabolic intermediates generated from the AA metabolism pathway further confirmed the role of these enzymes in ROP, while metabolites for *EPHX2* activity were low in abundance. Inflammatory lipid intermediates were higher compared to anti-inflammatory lipids in VH and showed an association with enzyme activity. Both the placenta of preterm infants who developed ROP and hypoxic retinal cultures showed a reduced expression of *EPHX2*. These findings suggested a strong involvement of *EPHX2* in regulating retinal neovascularization and inflammation. The study results

**Abbreviations:** AA, arachidonic acid; ALOX, activator of LOX; APH1B, Aph-1 homolog B; BV, blood vessels; CASP, caspases; COXs, cyclooxygenases; CYP1B1, cytochrome P450 family 1 subfamily B member 1; CYP2C8, cytochrome P450 family 2 subfamily C member 8; DHA, docosahexaenoic acid; DLL4, delta-like ligand4; DMEM, Dulbecco's Modified Eagle's Medium; EETs, eicosatetraenoic acid; ELM, external limiting membrane; EPA, eicosapentaenoic acid; EPHX2, epoxide hydrolase2; GCL, ganglion cell layer; GFAP, glial fibrillary acidic protein; H&E, hematoxylin and eosin; HETEs, hydroxy eicosatetraenoic acids; HIF1A, hypoxia-inducible factor 1 alpha; IHC, immuno-histochemistry; INL, inner nuclear layer; IPL, inner plexiform layer; LA, linoleic acid; LCMS, liquid chromatography mass spectrometry; LOXs, lipoxygenases; LTs, leukotrienes; NFL, nerve fiber layer; OIR, oxygen-induced retinopathy; ONL, outer nuclear layer; OPL, outer plexiform layer; PBS, phosphate buffer saline; PGs, prostaglandins; PSEN1, presenilin 1; PUFAs, polyunsaturated fatty acids; ROP, retinopathy of prematurity; RPE, retinal pigment epithelium; RRID, research resource identifiers; TXA2, thromboxane A2; VEGF, vascular endothelial growth factor; VEGFR, vascular endothelial growth factor receptor; VH, vitreous humor.

  

of Science and Technology, Ministry of Science and Technology, India, Grant/Award Number: IF190699; Hyderabad Eye Research Foundation, Grant/Award Number: LEC02-14-029

underscore the role of arachidonic acid metabolism in the development of ROP and as a potential target for preventing vision loss among preterm-born infants.

**KEYWORDS**
angiogenesis, arachidonic acid, inflammation, lipid, retinopathy of prematurity, soluble epoxide hydrolase

## 1 | INTRODUCTION

Retinopathy of prematurity (ROP) is a major ocular complication of preterm birth among children and is characterized prominently by abnormal blood vascularization and neurodegeneration in the retina, that eventually leads to fibrovascular proliferation and retinal detachment, causing total vision loss very early in life. Approximately 10%–18% of preterm infants born annually in high-income countries and 40% in low- and middle-income countries develop ROP, of which about 18% have significant vision loss (Blencowe et al., 2013; Rivera et al., 2017; Sanghi et al., 2018). Preterm infants, once diagnosed with plus ROP (characterized by the development of abnormal blood vessels on a partial avascular retina), are treated with laser and/or anti-VEGF (Vascular Endothelial Growth Factor) therapy (Hartnett, 2015). Currently available treatment options for ROP mainly aim at preventing the progression of the disease with some known side effects and show variable responses to retinal maturation and functions. Besides, preterm infants who develop ROP are at a higher risk of developing secondary ocular complications, including retinal detachment, myopia (nearsightedness), strabismus (crossed eyes), amblyopia (lazy eyes), and glaucoma. Many studies attempted to demonstrate the underlying cellular and molecular mechanisms in the pathogenesis of ROP, but it is still not fully understood (Kaur et al., 2022; Rivera et al., 2017). Moreover, it is yet unclear why only a subset of mild ROP cases progress to severe ROP while in others the disease spontaneously regresses to mature retina and the role of maternal factors. Mounting evidence thus far has indicated a complex interplay between metabolism and pathways regulating hypoxia, inflammation, and angiogenesis (Chen & Smith, 2007; Fu et al., 2022; Hartnett & Lane, 2013; Patnaik et al., 2021).

The deficiency of ω-3 polyunsaturated fatty acids (PUFAs), particularly DHA (docosahexaenoic acid), has been reported as a potential contributor to ROP pathology (Fu et al., 2022; Lapillonne & Moltu, 2016). Several randomized control trials performed on PUFA supplementation for preterm infants showed a trend toward benefit in mitigating severe forms of ROP; however, there was no change observed after a prolonged follow-up for the visual acuity at the age of 2.5 years (Liu et al., 2013; Welch et al., 2007). Plausibly, this could be as a result of the non-consideration of PUFA metabolizing enzymes and PUFA metabolism. The macular layer in the retina is rich in long-chain PUFAs such as arachidonic acids (AA), DHA, eicosapentaenoic acid (EPA), etc., which are prone to frequent lipid peroxidation and structural modification leading to the loss of neurons (Wang et al., 2019). The role of PUFAs and lipid-metabolizing enzymes such as cyclooxygenases, lipoxygenases, and hydrolases has been widely studied in cancer and cardiovascular diseases; however, their involvement in ROP has been less explored. An increased activity of COXs (Cyclooxygenases) and LOXs (Lipoxygenases) on AA generates prostaglandins (PGs), thromboxane A2 (TXA2), leukotrienes (LTs), and hydroxy eicosatetraenoic acid (HETEs), which are known to contribute to inflammation and hypertension (Snodgrass & Brune, 2019; Zemski Berry et al., 2014). Further, AA is also acted upon by a group of CYPs (Cytochrome P450) enzymes (ω-hydroxylases and epoxygenase pathways) generating HETEs and eicosatetraenoic acid (EETs), which regulate some cellular processes of carcinogenesis and progression, including cell proliferation, survival, angiogenesis, invasion, and metastasis. The EETs are mainly metabolized by soluble epoxide hydrolase (sEH/EPHX2) to the corresponding diols or dihydroxyeicosatrienoic acids (DHETs). Hypoxia is extensively explored as a major factor in the development and progression of ROP and has a significant association with abnormal fatty acid metabolism. However, the role of PUFA-metabolizing enzymes in regulating angiogenesis has not been explored in human patients. Recently, a few studies using oxygen-induced retinopathy mouse models have shown the prominent role of EPHX2, a major enzyme in the AA metabolism, in astrocyte and endothelial cell proliferation, leading to new vessel growth in the retina (Hu et al., 2019). Further, the reports on the role of EPHX2 are variable, and it is unclear if they confer protection or contribute to abnormal angiogenesis under hyperoxia/hypoxia. Based on the available literature and preliminary data on global gene expression data from ROP infants, we hypothesized that loss of EPHX2 activity in the growing retina alters PUFA metabolism, leading to abnormal angiogenesis via Notch signaling. Thus, the present study is an attempt to systematically understand the role of lipid-metabolizing enzymes in the AA pathway in contributing to abnormal angiogenesis and neuronal loss in ROP. This was achieved by integrating targeted transcriptomics and fatty acid metabolomics in premature infants. The study also attempts to understand the interplay between cellular and signaling pathways regulating lipid metabolism, inflammation, angiogenesis, and neurodegeneration in ROP development and progression by analyzing multiple tissue types such as blood, vitreous humor (VH), preterm retina, and placenta. Aberrant fatty acid metabolism among preterm-born infants may be a key event in the development and progression of ROP, and, thereby, could offer a major therapeutic option for ROP.

## 2 | MATERIALS AND METHODS

### 2.1 | Study subjects

The study protocol adhered to the principles of the Declaration of Helsinki and was approved by the Institutional Review Board (LEC-BHR-P-11-22-959) for VH, retina, and blood (LEC-BHR-01-20-380 for placental samples) of the L V Prasad Eye Institute (LVPEI), Hyderabad. Preterm babies referred for further management from the neonatal intensive care units across the city to the LVPEI were enrolled in the study. The study cohort for blood samples comprised 126 preterm infants of GA ≤35 weeks and/or BW ≤1700 g with severe ROP ($n=70$) and no/mild ROP ($n=56$). The study cohort for VH samples comprised 15 preterm babies with severe ROP and 15 controls with GA ≥35 weeks and/or BW ≥2500 with congenital cataracts. The inclusion and exclusion criteria for placenta sample collection are provided in Table T2 and are also mentioned in detail in another manuscript (Kaur et al. bioRxiv 2023.02.13.528236). The included preterm infants were thoroughly examined by an ophthalmologist on the 21st day of life for retinal vascular status as part of the routine screening done by the retina specialists of LVPEI. Based upon the examination, the preterm infants were further divided into preterm without ROP and preterm with ROP groups. The detailed demographic and clinical history of all the infants/patients recruited for the study was documented in a pre-designed proforma, and written informed consent was obtained from their guardians prior to the sample collection.

#### 2.1.1 | Criteria applied for the diagnosis and progression of ROP

Diagnosis and categorization of ROP cases were done based on severity (stages 1–5), location (zones I, II, and III), amount of disease (clock hours), and presence or absence of "plus" disease following ICROP guidelines. Severe ROP includes progressive disease and a highly vascularized retina, which requires prompt treatment. The no/mild ROP cases include less severe disease, which does not require any treatment and has no neo-vascularization changes. The preterm infants with no/mild ROP and no neo-vascularization changes in the retina were considered control, while infants with stage 4 and stage 5 plus who had severe neo-vascular changes and/or retinal detachment were categorized as severe ROP in this study. All infants enrolled in the study were regularly followed for disease status until the disease completely regressed. Infants on steroid treatment and with a history of anti-VEGF were excluded. In addition to blood samples and VH, placenta samples from preterm and full-term-born infants (at the time of delivery) and retina tissue (at the time of evisceration) were also collected from a subset of patients for understanding the lipid metabolism in utero and in severe stages of ROP, respectively. Infants included for placenta analysis were thoroughly examined and followed up for at least six months for the development of ROP/normal vascularization.

### 2.2 | Sample collection

Venous blood (0.5–1.5 mL) was collected from the preterm infants diagnosed with severe ROP and controls by venipuncture. Placental tissue (decidua representing the maternal–fetal interface) was collected based on gestational age as per study criteria and categorized into preterm ($n=6$) and full-term ($n=3$). RNA was extracted from the blood and placental samples using Trizol and an automated cDNA extraction platform following the manufacturer's guidelines. Likewise, for metabolomics studies, the VH samples (400 μL) were collected from preterm infants with stage IV and V ROP ($n=15$) who had undergone vitrectomy as a part of their routine clinical management. All the infants enrolled in this study had a minimum of 6 h of fasting prior to the surgery to normalize the effect of external nutrition on their metabolic profile (Toms & Rai, 2019). The controls for the metabolomics studies included infants with congenital cataracts (<6 months of age) who underwent partial vitrectomy as part of their surgical management ($n=15$). The mean age at the VH sample collection was non-significant to minimize its maturation time post-birth. Retina from patients with ROP and an age-matched control with anterior staphyloma was collected during evisceration.

### 2.3 | Materials

All the primers for semi-quantitative PCR were synthesized by Bioserve Biotechnologies (India) Pvt Ltd. The rabbit polyclonal antibody against EPHX2 (RRID:AB_10263545) was purchased from R&D Biosystems Inc. (RRID:SCR_006140), and the mouse monoclonal antibody anti-Glial fibrillary acidic protein (GFAP; RRID:AB_2314537) was purchased from Cell Signaling Technology (RRID:SCR_002071) for immunohistochemistry (IHC). Secondary antibodies for IHC were from LI-Cor Biosciences. All other chemicals (unless otherwise specified) were from Sigma-Aldrich (RRID:SCR_008988).

### 2.4 | Reverse transcription and semi-quantitative PCR

RNA from blood samples of severe ROP and no/mild ROP was extracted by the QIAamp RNA Blood Mini kit method (QIAGEN (RRID:SCR_008539); Hilden, Germany). The RNA from the placenta and human primary retinal cell culture was extracted using TRIzol. The quantity and quality of extracted RNA were assessed by Thermo NanoDrop (concentration range = 100–1000 mg/μL, A260/230 = 2.0 ± 0.05). cDNA was prepared using the iScript cDNA synthesis kit (Bio-Rad Laboratories (RRID:SCR_008426), CA, USA). Semi-quantitative PCR was carried out using the specific primers for AA metabolism genes (*CYP1B1*, *CYP2C8*, *COX2*, *ALOX15*, and *EPHX2*), angiogenic genes (*VEGF165/189*, *VEGFR2*, *DLL4*, *PSEN1*, *APH1B*, and *NOTCH1*), hypoxia-inducible factor gene (*HIF1A*), and cell death marker genes (*CASP3 and CASP8*). All primers were designed using Primer3 software (RRID:SCR_003139). The expression

of each gene was normalized to that of β-*actin* as an endogenous control (Table S1).

## 2.5 | IHC and hematoxylin and eosin (H&E) staining of retina

To determine the expression of EPHX2 and GFAP in ROP eyes from preterm infants, retinal tissue from ROP and an age-matched control were collected at the time of evisceration. The retinal tissues were washed with 1X PBS thrice. The sclera, choroid, retinal pigment epithelium (RPE), Buch's membrane, along with vessels in these layers, was removed and the neural retina was immersed in 4% formalin for 24 h. The tissue was later embedded in a paraffin block and stored until use. The tissue section of 10 μm from the paraffin block was made on a charged glass slide and deparaffinized. Sections were cut, air dried, and stained with H&E (Fischer et al., 2008) to understand their morphology. The antigen retrieval was performed using ammonium acetate buffer, followed by brief heating. For whole-mount IHC, the retina was fixed in 4% paraformaldehyde (PFA) for 20 min at room temperature and washed with PBS buffer thrice. After isolation, tissues were blocked and permeabilized in 2% BSA and 0.5% Triton X-100 at room temperature for 1 h. The primary antibodies for EPHX2 (1:300) and GFAP (1:300) were diluted in 2% BSA and kept at 4°C overnight. Afterward, Alexa Fluor–coupled secondary antibodies (1:300) were used. Cell nuclei were visualized with DAPI (1:200; Molecular Probes, Thermo Fisher Scientific USA). Human skin was used as a positive control for EPHX2 (SF2) (Naeem et al., 2024). All high-resolution images were visualized and captured with a confocal microscope (Carl Zeiss AG, Oberkochen, Germany; Scale: 20 μm).

## 2.6 | Preparation of human mixed retinal cell cultures and hypoxia induction

The detailed human mixed retinal cell cultures were established from cadaveric donor retinas, as previously explained (Shahulhameed et al., 2020; Institutional Review Board: LEC 02-14-029). Briefly, retinal tissue was chopped into small pieces with the help of a sterile surgical blade and then washed with 1X PBS. The dissociated pieces of retina were subjected to trypsinization using 1X trypsin EDTA (0.25%) for 15 min at 37°C. The reaction was stopped by adding a complete DMEM (Dulbecco's Modified Eagle's Medium) containing 10% serum and 1% antibiotics, followed by resuspending these in 2 mL of PBS and gently mixing. The tubes containing resuspended cells were centrifuged, and the supernatant was removed to obtain a clear cell pellet, which was again suspended in DMEM. The suspended cells were then seeded in a sterile tissue culture grade T-75 mm flask and left undisturbed under standard cell culture conditions for 7 days, with the medium changing every third day. The newly grown cells were seeded ($n = 15000$/well) on a glass coverslip and allowed to grow for 70%–80% confluency; 150 μM of $CoCl_2$ was used for 24 h in serum-deprived medium to induce hypoxia. The unexposed cells in a serum free medium (24 h) were used as a control. After hypoxia treatment, the cells were isolated for RNA extraction.

## 2.7 | Metabolomics analysis

Global VH metabolome data for ROP and controls were generated in our lab using the previously described protocol (Kumar et al., 2023; Patnaik et al., 2019). The VH samples collected during surgery were kept on ice and immediately brought to the lab, and metabolite extraction was performed within 30 min, snap-frozen in liquid $N_2$, and then stored at −80°C until further use. All the samples were run in triplicate, and the metabolites were considered for analysis only if they were present in more than 80% of all the samples and replicates to maintain quality control. Further, we have performed baseline correction with the blank prior to injecting the sample and running the blank in between the runs. The mass spectrometry was calibrated, and tuning was done frequently between runs to achieve adequate quality control for the data generated. The abundance value underwent a $\log_2$ transformation. The dataset was further mined for lipid-specific metabolites with a 15-ppm difference for annotation using XCMS (RRID:SCR_015538), and identified in the Human Metabolome Data Bank (HMDB; RRID:SCR_007712). Metabolites generated by the activity of AA pathway genes were mapped, and a predictive analysis for the *EPHX2* gene and its interactions with AA-derived metabolite {LC–MS (liquid chromatography-mass spectrometry) data} was performed using the MetScape-Cytoscape analysis tool.

## 2.8 | Statistical analysis

The data are represented in terms of the mean and the standard error mean (SEM). The significance of the differences between the groups was analyzed using the two-tailed Student's *T*-test. The qPCR expression was determined using cycle threshold ($C_t$) values calculated for each test gene obtained for each sample using SDS2.3 software, and the mean fold change was calculated using $2^{-\Delta\Delta Ct}$. We have calculated the relative mRNA expression based on fold change by using individual $\Delta C_t$ of the control and severe ROP following recent published articles (Diebold et al., 2019; Harshitha & Arunraj, 2021). To study the variance among the categories, the degree of freedom, *t*-value, *F*-value, and actual *p*-value were calculated. For IHC quantification, we utilized ImageJ Fiji software. Lipid metabolites were annotated using the Metlin XCMS online tool in both positive and negative ion adduct mode (http://metlin.scripps.edu). The post-hoc power analysis for determining the effect size for this study was performed using a dichotomous endpoint and two independent sample groups based on the incidence of severe ROP in India (https://clincalc.com/stats/Power.aspx) and showed a score of 92.5%. The data were not assessed for normality, and no test for outliers was conducted. Statistical significance was considered at $p \leq 0.05$. Statistical analyses were carried out using GraphPad Prism version 9.0.0 (RRID:SCR_002798).

## 3 | RESULTS

### 3.1 | Study cohort

A total of 126 preterm infants were recruited and analyzed for gene expression profiling. Table 1 provides the demographic details for all the study subjects. The blood sample cohort showed severe ROP infants had significantly lower gestational age and birth weight as compared to those with no/mild ROP. The study population for the metabolomics study from VH samples included 30 infants (ROP: 15; controls: 15).

#### 3.1.1 | Targeted gene expression profiling among severe ROP and control cases shows significant alterations in the expression of the enzymes involved in AA metabolism

Taking a cue from our earlier results obtained from a previous published study on proteomics and genomics analysis of ROP (Rathi et al., 2017) and to have a detailed understanding of the role of AA metabolism in ROP pathogenesis, we first compared the expression of key genes in this pathway, including *COX2*, *ALOX15*, *CYP1B1*, *CYP2C8*, and *EPHX2*, among preterm infants with severe ROP and control (Figure 1). Four of the prominent genes/enzymes involved in AA metabolism, including *COX2*, *ALOX15*, *CYP1B1*, and *CYP2C8*, were significantly upregulated (2.5-fold, $p=0.05$; 3.9-fold, $p=0.03$; 5.8-fold, $p=0.007$; and 2.0-fold, $p=0.05$, respectively), while *EPHX2* was significantly downregulated (0.56-fold, $p=0.04$; Figure 1).

**TABLE 1** Demographic details of the patients recruited.

| Variable | Severe ROP | Control/ mild ROP | *p*-value |
|---|---|---|---|
| (a) Blood | | | |
| Total infants, *n* | 70 | 56 | - |
| Male, *n* (%) | 37 (52.8) | 33 (58.9) | - |
| Female, *n* (%) | 33 (47.2) | 23 (41.1) | - |
| Mean BW (in grams)<br>SD | 1309.1<br>398.17 | 1514.4<br>415.6 | 0.00623 |
| Mean GA (in months)<br>SD | 29.08<br>2.03 | 32.10<br>2.20 | <0.00001 |
| (b) VH | | | |
| Total infants, *n* | 15 | 15 | - |
| Male, *n* (%) | 7 (46.7) | 9 (60) | - |
| Female, *n* (%) | 8 (53.3) | 6 (40) | - |
| Age (in months) at the time of surgery<br>SD | 3.83<br>1.12 | 3.4<br>1.7 | n.s. |

*Note*: (a) Details of the patients and controls recruited for gene expression profiling in blood. (b) Details of the patients and controls recruited for the metabolite profiling in the VH.

Abbreviations: BW, birth weight; GA, gestational age; n.s, non-significant; ROP, retinopathy of prematurity; SD, standard deviation.

#### 3.1.2 | Reduced expression of EPHX2 further dysregulates angiogenic genes via upregulating notch signaling

*EPHX2* is known to regulate Notch signaling, which in turn regulates angiogenesis and cell death. Therefore, to confirm the reduced expression of *EPHX2* and its implication in ROP, we compared the quantitative expression of angiogenic genes, *VEGF165*, *VEGF189*, *PSEN1*, *APH1B*, *DLL4*, and *NOTCH1* in preterm infants with severe ROP and with no/mild ROP (Figure 2). Pro-angiogenic genes, including *VEGF165* and *VEGF189* and its receptor VEGFR2 showed increased expression (6.0-fold, $p=0.001$; 5.7-fold, $p=0.02$; 14.5-fold, $p=0.007$). The γ-secretase component, which cleaves the notch receptor, *APH1B*, was significantly upregulated (2.3-fold, $p=0.035$, respectively), while *PSEN1* was significantly (0.4-fold, $p=0.04$) downregulated. *DLL4*, which is a ligand for notch activation and negatively regulates VEGF, did not show any change. *NOTCH1*, which acts as a regulator of angiogenesis, was also significantly (3.0-fold, $p=0.003$) upregulated.

The gene expression of apoptotic genes, *CASP3* and *CASP8* was assessed among severe ROP and control samples (Figure 3). Both *CASP3* and *CASP8* were significantly upregulated (2.2-fold, $p=0.01$- and 1.5-fold, $p=0.004$). Hypoxia-inducible factor 1A (HIF1A) was significantly increased in cases (8.4-fold, $p=0.0009$). These results clearly suggest that a reduced expression of *EPHX2* affects its major activity of converting EETs to DHETs, which might further contribute to neovascularization via notch signaling. Also, increased EETs would further increase VEGF.

### 3.2 | Functional implications of differential expression of lipid-metabolizing enzymes in the eyes of ROP patients

Next, to assess the functional effect of differential expression of lipid-metabolizing enzymes on retinal pathology, their activity was estimated from the metabolites generated in the VH samples of ROP patients and controls. These data generated in our lab are being analyzed to identify the key mechanisms involved in ROP pathogenesis (a manuscript *submitted to another journal*). Of the 1031 total identified metabolites in the VH, lipids constituted approximately 40% of the total differentially expressed metabolites among cases and controls. A total of 69 metabolites involved in fatty acid metabolic pathways showed differential expression between ROP and control (Figure 4a, Table 2).

#### 3.2.1 | Combined analysis of the *EPHX2* gene and metabolic interactions

To delineate the underlying mechanisms involving *EPHX2* in the pathogenesis of ROP, as shown above, an interactive map for the *EPHX2* gene and epoxy-derived metabolites was constructed using Metscape (Cytoscape plugin). The *EPHX2* gene has both direct and indirect

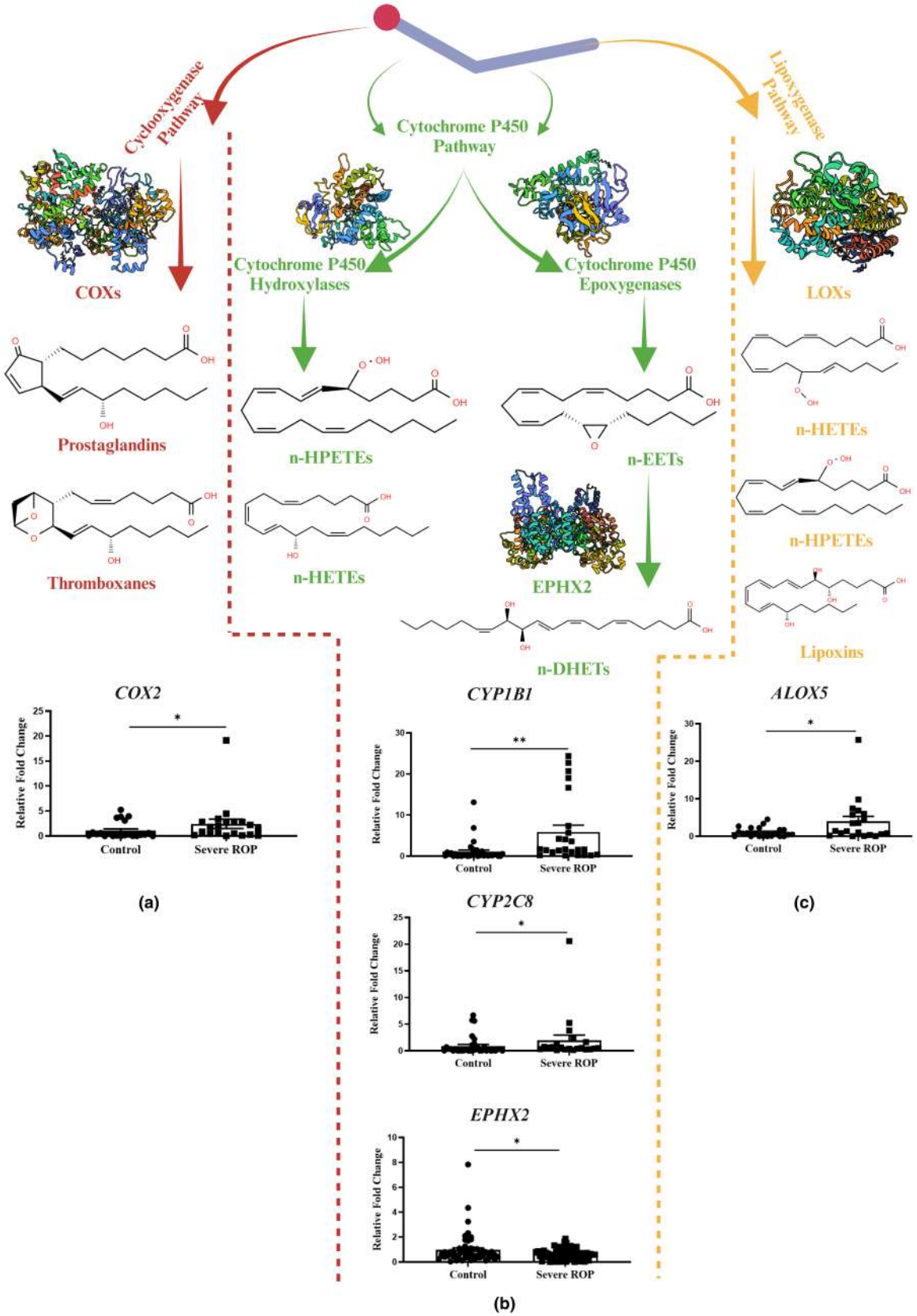
Cyclooxygenase Pathway
Cytochrome P450 Pathway
Lipoxygenase Pathway
COXs
Cytochrome P450 Hydroxylases
Cytochrome P450 Epoxygenases
LOXs
Prostaglandins
n-HPETEs
n-EETs
n-HETEs
Thromboxanes
n-HETEs
EPHX2
n-HPETEs
n-DHETs
Lipoxins
COX2
CYP1B1
ALOX5
Relative Fold Change
Control
Severe ROP
(a)
CYP2C8
EPHX2
(b)
(c)

**FIGURE 1** Arachidonic acid metabolism: Classification of different metabolites formed from AA by different enzymatic pathways. The cyclooxygenase and lipoxygenase pathways are mediated by the activity of COXs forming prostaglandins and thromboxanes and LOXs forming HETEs, HPETEs, and lipoxins, respectively. Epoxygenase and ω-hydroxylase pathways are mediated by the activity of CYPs, forming classes of EETs, HETEs, and HPETEs, respectively. EPHX2 acts on the epoxygenase-generated metabolites to form dihydroxy alcohols (n-DHETs). (a) qRT-PCR analysis of transcripts for *COX2* ($D_f = 42$; *t*-value = 2.01; $n = 21$ preterm babies with severe ROP; $n = 23$ preterm babies with no/mild ROP; $p = 0.0503$) (b) qRT-PCR analysis of transcripts for *CYP2C8* ($D_f = 59$; *t*-value = 2.01; $n = 25$ preterm babies with severe ROP; $n = 36$ preterm babies with no/mild ROP; $p = 0.0504$); *CYP1B1* ($D_f = 60$; *t*-value = 2.80; $n = 26$ preterm babies with severe ROP; $n = 36$ preterm babies with no/mild ROP; $p = 0.0072$); and qRT-PCR analysis of transcripts for *EPHX2* ($D_f = 124$; *t*-value = 2.07; $n = 70$ preterm babies with severe ROP; $n = 56$ preterm babies with no/mild ROP; $p = 0.0415$). (c) *ALOX15* expression ($D_f = 42$; *t*-value = 2.16; $n = 21$ preterm babies with severe ROP; $n = 23$ preterm babies with no/mild ROP; $p = 0.0503$). All the graphs are representative of experimental triplicates. β-Actin was used as the normalization control for qRT-PCR. Statistical significance is represented as * and ** for $p \leq 0.05$ and $p \leq 0.01$, respectively.

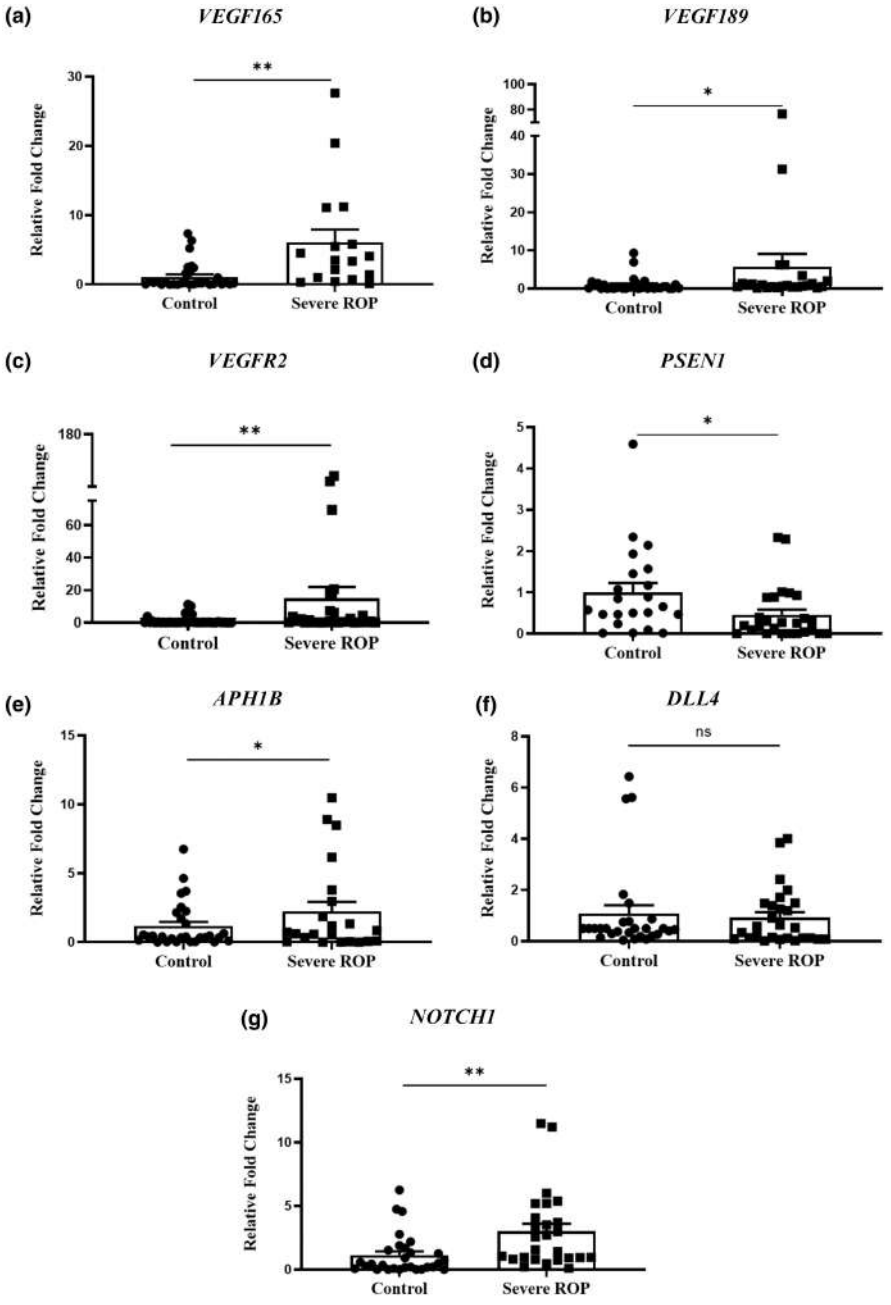


**FIGURE 2** mRNA expression levels of angiogenic genes in blood: (a) qRT-PCR analysis of transcripts for *VEGF165* ($D_f = 49$; *t*-value = 2.24; $n = 18$ preterm babies with severe ROP; $n = 33$ preterm babies with no/mild ROP; $p = 0.0265$; (b) *VEGF189* ($D_f = 48$; *t*-value = 3.42; $n = 17$ preterm babies with severe ROP; $n = 33$ preterm babies with no/mild ROP; $p = 0.00163$); (c) *VEGFR2* ($D_f = 66$; *t*-value = 3.42; $n = 30$ preterm babies with severe ROP; $n = 38$ preterm babies with no/mild ROP; $p = 0.00163$) expression; (d) qRT-PCR analysis of transcripts for *PSEN1* ($D_f = 50$; *t*-value = 2.07; $n = 29$ preterm babies with severe ROP; $n = 23$ preterm babies with no/mild ROP; $p = 0.0474$); (e) *APH1B* ($D_f = 54$; *t*-value = 2.19; $n = 26$ preterm babies with severe ROP; $n = 30$ preterm babies with no/mild ROP; $p = 0.0355$) expression (f) qRT-PCR analysis of transcripts for *DLL4* ($D_f = 66$; *t*-value = 0.634; $n = 38$ preterm babies with severe ROP; $n = 30$ preterm babies with no/mild ROP; $p = 0.5308$) (g) qRT-PCR analysis of transcripts for *NOTCH1* ($D_f = 54$; *t*-value = 3.08; $n = 26$ preterm babies with severe ROP; $n = 30$ preterm babies with no/mild ROP; $p = 0.0039$). All the graphs are representatives of experimental triplicates. β-Actin was used as the normalization control for qRT-PCR. Statistical significance is represented as * and ** for $p \leq 0.05$ and $p \leq 0.01$, respectively.

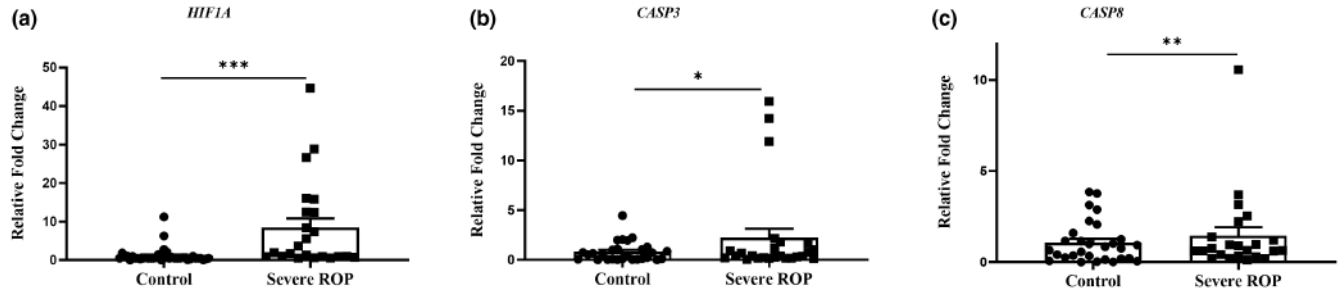


FIGURE 3 mRNA expression levels of hypoxia-inducible factor and apoptotic genes in blood: (a) qRT-PCR analysis of transcripts for *HIF1A* ($D_f = 66$; $t$-value = 3.58; $n = 30$ preterm babies with severe ROP; $n = 38$ preterm babies with no/mild ROP; $p = 0.00095$) expression; (b) qRT-PCR analysis of transcripts for *CASP3* ($D_f = 56$; $t$-value = 2.51; $n = 27$ preterm babies with severe ROP; $n = 31$ preterm babies with no/mild ROP; $p = 0.0156$); (c) *CASP8* ($D_f = 53$; $t$-value = 3.05; $n = 25$ preterm babies with severe ROP; $n = 30$ preterm babies with no/mild ROP; $p = 0.00423$) expression. All the graphs are representative of experimental triplicates. β-Actin was used as the normalization control for qRT-PCR. Statistical significance is represented as * and ** for $p \le 0.05$ and $p \le 0.01$, respectively.

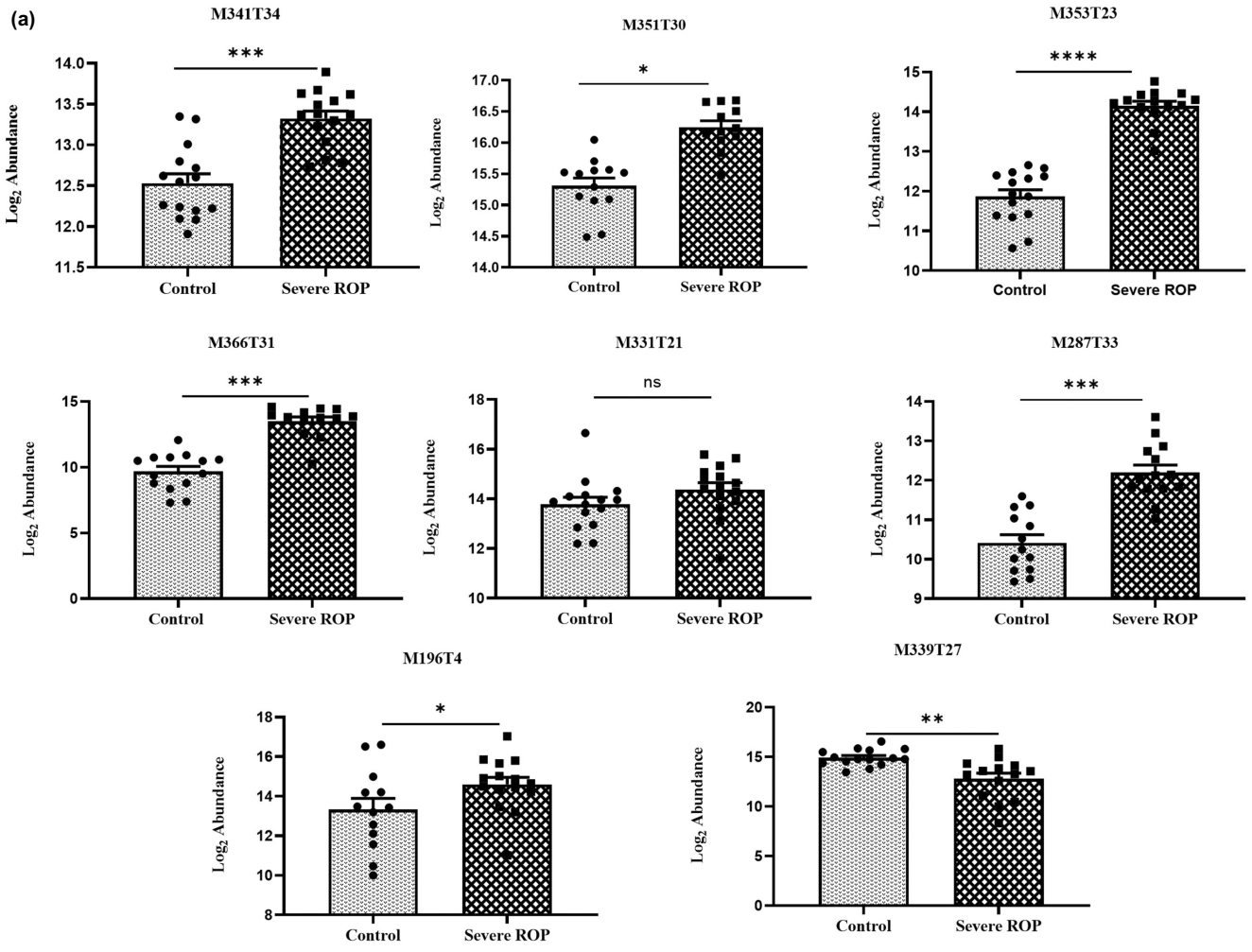


FIGURE 4 AA metabolites found in VH and lipid metabolite interactions with its genes: (a) Abundance of fatty acid metabolites in the VH. The graphical representation of the abundance of metabolites detected in the VH of severe ROP compared to control. The corresponding $x$-axis represents the Metline ID for the metabolites detected. $n = 15$ preterm babies with severe ROP; $n = 15$ full-term babies with no ROP. (b) Network mapping of EPHX2 and lipid-derived metabolites: the EPHX2 gene showing strong association with CYPs and other lipid-metabolizing enzymes. (c) Network mapping of CYP450 and lipid-derived metabolites: Different CYP450 family gene interactions with its metabolites. The network map shows the interactions among different metabolites and their associations with the genes mapped. All the graphs are representatives of biological duplicates. All graphs were prepared using GraphPad Prism version 9.0.0. Statistical significance is represented as *, **, and *** for $p \le 0.05$, $p \le 0.01$, and $p \le 0.001$, respectively.

Journal of Neurochemistry JNC The Official Journal of the International Society for Neurochemistry WILEY



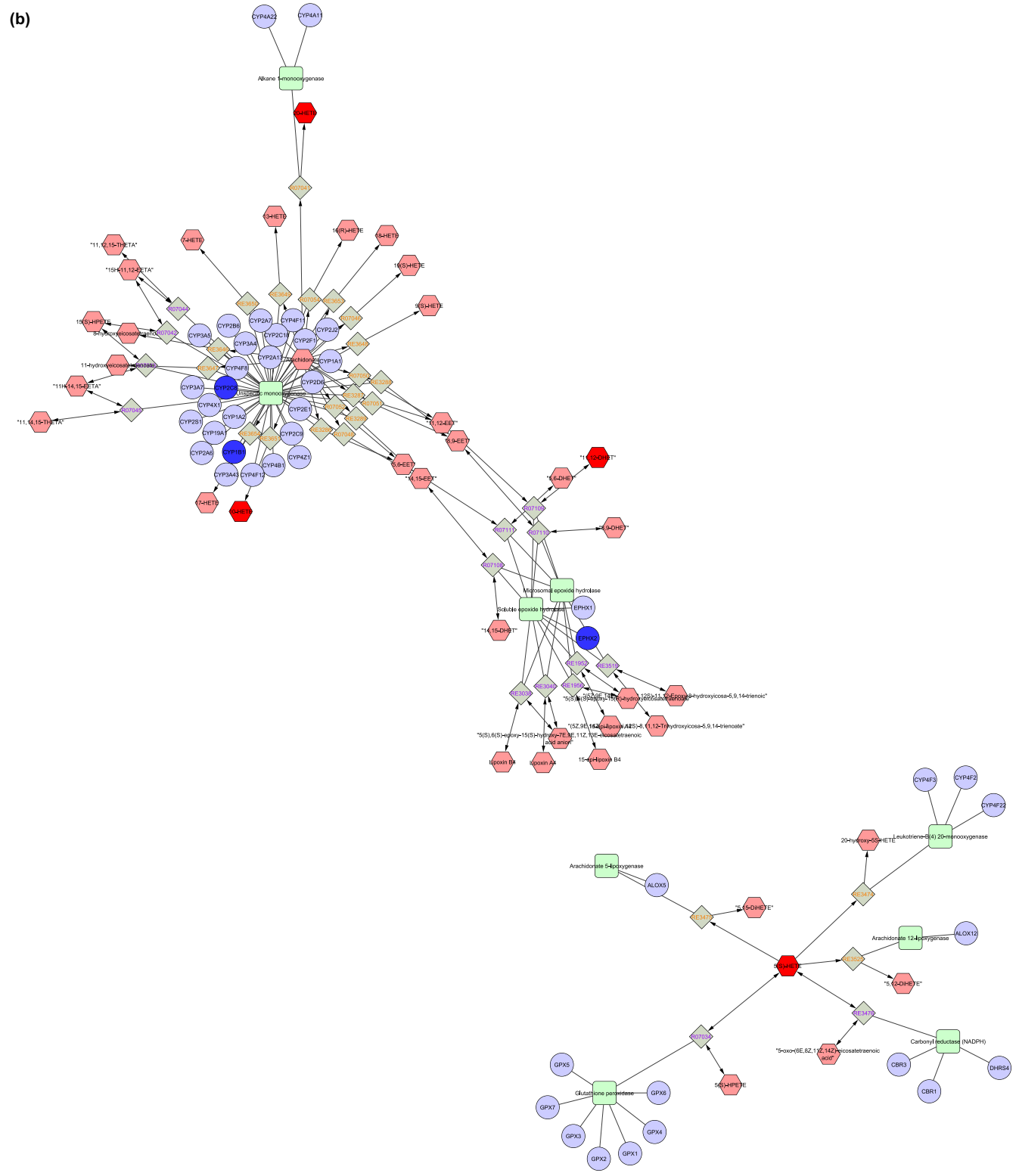


FIGURE 4 (Continued)

interactions with several pro-inflammatory metabolites and CYP genes (*CYP1B1*, *CYP2C8*, etc.). Most of these interactions are involved in the different lipid metabolic pathways, namely AA metabolism, di-unsaturated fatty acid beta-oxidation, leukotriene metabolism, linoleate metabolism, putative anti-inflammatory metabolite formation from EETs, and xenobiotic metabolism pathways (Figure 4b,c).

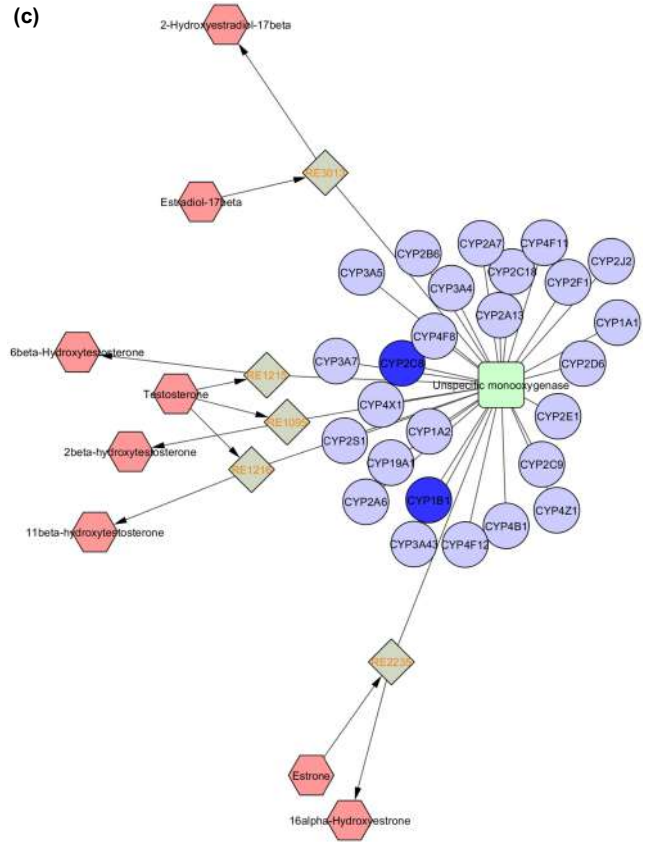


FIGURE 4 (Continued)

### 3.3 | Expression of EPHX2 is modulated by hypoxia in vitro and in utero

We next assessed if the reduced expression of the *EPHX2* is triggered or regulated by hypoxia by exposing primary retinal cells to hypoxia (Figure 5). The expression of *EPHX2* gene in human primary mixed retinal culture showed a downregulation under hypoxia as compared to normal oxygen-supplemented cultures (0.11-fold, $p$-value = 0.002). Further, since the placenta provides oxygen and nutrition in utero, we tested if compromised growth/anatomical changes in the placenta leading to ischemia could modulate the *EPHX2* expression, which may predispose these infants to develop ROP postnatally. Compared to the placenta from a full-term delivery, expression of *EPHX2* was reduced in the placenta from preterm delivery who did not develop ROP (Figure 5); however, it was significantly reduced for those who developed ROP (fold change = 0.16; $p$-value = 0.00003).

### 3.4 | Reduced EPHX2 expression in the severe stage of ROP retina corroborates its role in ROP pathogenesis

Next, we assessed the retinal structural and morphology on H&E staining in the retina from a control and severe stage of a human preterm infant, which showed proper retinal layers in the control retina as compared to the ROP retina. The H&E section of the ROP retina showed loss of lamination (arrangements of photoreceptors, neurons, and other cell types in different layers), gliosis with more fibrotic cells, and vascular proliferation. Clearly, the retinal layers in ROP sections were indistinguishable compared to the controls. These phenotypic changes could be attributed to the altered metabolite levels and high inflammation. Lastly, we tested if the altered expression of EPHX2 could potentially lead to the progression of ROP by checking its expression in the astrocytes and other glial cells of retinal sections. An intense positive staining of the astrocyte/glial marker GFAP was seen in the ROP retina, which was relatively higher than that seen in the control retina. EPHX2 showed no expression in the retina in ROP subjects with very few neuronal cells. Among the control retina sections, a higher expression of EPHX2 was observed near the blood vessel region (yellow arrow) with astrocytic cells expressed in GCL and NFL (Figure 6).

## 4 | DISCUSSION

Multiple key factors, including oxidative stress, inflammation, neovascularization, and apoptosis, are known to affect the overall development and maturation of the retina in preterm-born infants and contribute to ROP pathogenesis (Hartnett & Lane, 2013; Rivera et al., 2017). In this study, we have shown that these factors are modulated by several lipid-metabolizing enzymes and angiogenic genes. The expression of genes coding for the major enzymes in the AA pathway, *COX2*, *ALOX5*, *CYP2C8*, and *CYP1B1* showed a significant upregulation at severe stages, along with their increased activity as reflected by the increased metabolite levels of inflammatory prostanoids such as PGs, Prostaglandin B2, Thbx, LTs, Leukotriene B5, Lipoxin B4, 11,12-EETs, and HETEs (first-order metabolites of AA pathway) in the ROP VH (Table 2; Figure 4). Previously, it was shown that EETs metabolism upon the induction of COX-2 tends to be proangiogenic in endothelial cells and might be mediating its proangiogenic activity through the VEGFR-2/3 signaling pathway by positive feedback of VEGF (Cheranov et al., 2008; Rand et al., 2019; Webler et al., 2008). The results of the present study confirm the same among ROP and no-ROP preterm infants.

Further, the present study also demonstrated a reduced *EPHX2* expression yielding low PUFA-derived diols (5,6 DHET and 8,9 DHET; Table 2). *EPHX2*-derived diols are required to protect astrocytes from mitochondrial-mediated apoptosis to prevent the development of ROP (Hu et al., 2014; Hu et al., 2019). Studies by Hu et al. also suggested that supplementation of 19,20-DHDP, but not the parent epoxide, was able to rescue the defective angiogenesis in $sEH^{-/-}$ mice. Interestingly, among diabetic retinopathy (DR) cases, the inhibition of sEH was reported to prevent or delay the DR progression (Hu et al., 2017). It is well known that sEH is a bifunctional enzyme (N-terminal has phosphatase activity and C-terminal has epoxygenase activity), and its expression can be altered under phase I and phase II of ROP development

**TABLE 2** List of metabolites and their corresponding METLIN IDs observed against peak is observed in the VH. XCMS-derived METLIN ID annotated against their retention time and with 15 ppm error was used for the analysis, and the identified features were both analyzed in positive mode and negative mode.

| METLIN ID | Retention time | m/z | Metabolites | Enzyme involved | Fold change | *p*-value | *t*-value | Degree of freedom ($D_f$) |
|---|---|---|---|---|---|---|---|---|
| M341T34 | 27.06 | 335.22 | (15S)-Prostaglandin A2; Prostaglandin B2; Prostaglandin-C2; Delta-12-Prostaglandin J2; AA (hydroperoxide); Leukotriene B5 | LOXs/COXs | 1.69 | <0.001 | 5.42 | 28 |
| M351T30 | 29.59 | 351.25 | 9-deoxy-9-methylene-PGE2; 11-deoxy-11-methylene-PGD2; PGA1 methyl ester; 5-HETE methyl ester | COXs/ non-enzymatic | 1.74 | 0.02 | 5.73 | 23 |
| M353T23 | 23.21 | 353.22 | 13,14-Dihydro-15-keto-PGD2, DG [PGE2]; 8-iso-15-keto-PGF2a; Prostaglandin E2; 13,14-Dihydro-15-keto-PGE2; Lipoxin B4 | LOXs/COXs | 4.32 | <0.0001 | 10.88 | 27 |
| M331T21 | 23.21 | 331.25 | Trihydroxy-9-octadecenoic acid; 9,10,13-TriHOME; 9,12,13-TriHOME | Non-enzymatic | 1.3 | n.s. | 1.51 | 28 |
| M366T31 | 31.43 | 366.32 | Prostaglandin F1a-d9 | COXs | 10.15 | <0.001 | 7.55 | 25 |
| M287T33 | 21.41 | 283.11 | 11,12-Epoxyeicosatrienoic acid (EETs) | CYPs | 1.71 | <0.01 | 6.30 | 25 |
| M196T4 | 33.35 | 287.22 | Hexadecanedioic acid | Non-enzymatic | 3.68 | <0.001 | 1.95 | 26 |
| M339T27 | 26.85 | 339.25 | 5,6-Dihydroxy-8,11,14-eicosatrienoic acid; 8,9-dihydroxy-5,11,14-eicosatrienoic acid (DHETs) | EPHX2/sEH | −2.75 | 0.002 | 3.64 | 27 |

*p*-value and fold change are denoted in the respective columns.

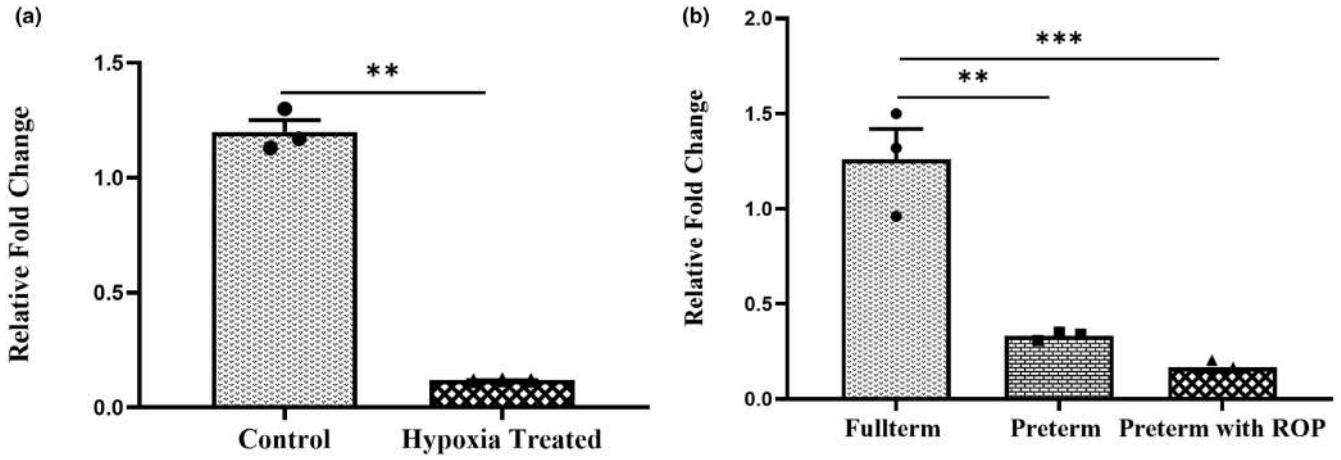


**FIGURE 5** Effect of hypoxia and prematurity on *EPHX2* expression: (a) qRT-PCR analysis of transcripts for *EPHX2* in human primary retinal culture under hypoxia. The hypoxia was induced using 150 μM $CoCl_2$, and the control was the primary culture exposed to normal room temperature oxygenation ($D_f = 4$; *t*-value = 21.05; $p = 0.0031$). For each independent experimental (3 biological set) set for human primary retinal culture, 15 000 cells/well were seeded. (b) qRT-PCR analysis of transcripts for *EPHX2* full-term placenta, $n = 3$; preterm placenta with no-ROP, $n = 3$; and preterm placenta from the infants who later developed ROP, $n = 3$. (One-way ANOVA; $F(2, 6) = 40.28$; $p = 0.0003$). All the graphs are representative of experimental triplicates. β-Actin was used as the normalization control for qRT-PCR. Statistical significance is represented as *, **, and *** for $p \leq 0.05$, $p \leq 0.01$, and $p \leq 0.001$, respectively.

(Harris & Hammock, 2013; Morisseau & Hammock, 2013). The N-terminal activity of sEH negatively regulates VEGF expression via nitric oxide synthase (Hou et al., 2012). An increased PGE2 (Table 2), as seen in this study, might be involved in mTORC activation leading to VEGF production, causing cell proliferation and angiogenesis, as shown in previous reports (Dufour et al., 2014; Wang et al., 2021). Likewise, based on the published reports by other groups (Luo et al., 2016; Nguyen et al., 2016; Spector & Norris, 2007), we speculate that increased EETs and HETEs formed by the activity of increased *CYP1B1* and *CYP2C8* may cause endothelial-mesenchymal transition leading to fibrosis as seen in the ROP retina (Figure 6). Further, exploring the angiogenic and VEGF pathways showed that the alterations in AA metabolites corroborate nicely with aggressive vascularization, as seen among severe ROP patients. We also found a significant upregulation of *HIF1A* (which regulates VEGF signaling) among severe ROP and controls. Hypoxic insults resulted in increased *HIF1A* expression in microglial cells, causing changes in cellular morphology and cell death (Dhyani et al., 2023). Concurrently, *VEGF165*, a pathogenic isoform of VEGF, was increased in comparison to *VEGF189* required for normal vascularization (Zhou et al., 2007). VEGF is known to activate and bind to different receptors to mediate its various effects. Binding of VEGF165 and VEGFR-2 was shown to be associated with pathologic features in a rat retinopathy model (Hartnett, 2015). This suggested that increased VEGF165 binding to increased VEGFR2 (Figure 2) may have significant implications in the vascular phases of human ROP. The results of the present study clearly demonstrated the same among ROP and no-ROP preterm infants. A high VEGF level increases several other inflammatory and proangiogenic factors, such as cytokines and ECM proteases, as revealed in our earlier findings (Patnaik et al., 2021; Rathi et al., 2017). Delta-like ligand 4 (Dll4) is induced by VEGF as a negative regulator of angiogenic sprouting; however, we did not see any significant change in *DLL4* expression. This could be explained based on the study by Lobov et al. (2007), which demonstrated that DLL4, which is known to act as feedback or "brake" for increasing VEGF, does not seem to regulate its expression at severe ROP (Lobov et al., 2007). Besides, Notch signaling may directly and/or indirectly regulate angiogenesis through crosstalk with VEFGRs (Garcia & Kandel, 2012; Hellström et al., 2007). DLL4, which is a ligand for the notch receptor, is cleaved by γ-secretases and ECM proteases (ADAM10); however, both act independently of each other (Hartmann et al., 2002; Hu et al., 2019; Sorensen & Conner, 2010). Further, other evidence from OIR models also showed a similar finding that DLL4 levels were not changed by fatty acid supplementation. However, the Notch cleavage is mediated by PSEN1 of γ-secretase activity (Hu et al., 2014). Differential expression of *PSEN1* and *APH1B* (both being components of γ-secretases; Figure 2) contributes to the cleavage of the notch, thereby increasing angiogenesis (Brunkan & Goate, 2005; Kopan & Ilagan, 2009). Notch, being a developmental pathway regulator, may be compromised among ROP infants because of an incomplete developmental cycle, as corroborated by relatively high-notch signaling. Increased hypoxia activates Notch-responsive promoters and increases expression of Notch-direct downstream genes (Gustafsson et al., 2005), which further strengthens the findings of our study.

Prematurity and oxidative insults are key factors in ROP progression and development, which were also assessed using in vitro human retinal primary cell culture models and placenta. Under both circumstances, *EPHX2* was seen downregulated. Maternal factors such as implantation, pregnancy, and labor are known to change

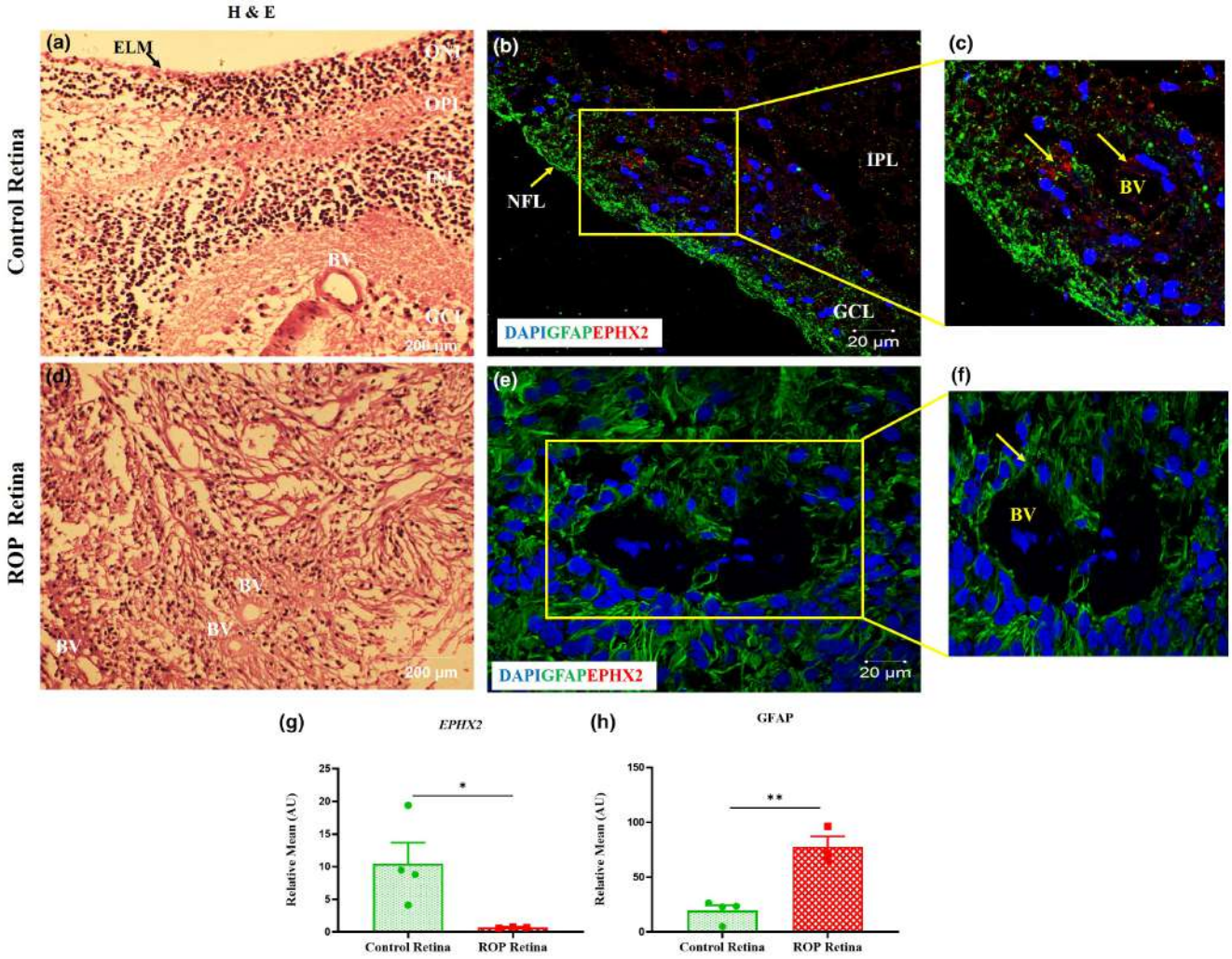


**FIGURE 6** (a) H&E staining of the control retinal panel showing different retinal layers and blood vessels. (Scale: 200 µm; Magnification: 20×; Microscope: EVOS M5000 Imaging System) (b) EPHX2 and GFAP expression in the control retina showing expression of GFAP in the blood vessels lining, near the NFL and GCL toward the VH, while EPHX2 expression is observed at the IPL and blood vessels lining. (c) Zoom-out section of the control retina showing the expression of EPHX2 colocalized with GFAP in the blood vessels lining. (d) H&E staining of the ROP retina shows no distinct retinal layer and loss of different retinal cells. (Scale: 200 µm; Magnification: 20×; Microscope: EVOS M5000 Imaging System) (e) EPHX2 and GFAP expression in the retina of ROP infants. The image shows an almost lack of expression of EPHX2, while significantly higher expression of GFAP across the retina. (f) Zoom-out section of the ROP retina showing very high expression of GFAP in the blood vessels lining but no expression of EPHX2 (g) Quantification of EPHX2 ($D_f = 5$; $t$-value = 2.56; $n = 3$ for ROP retina; $n = 4$ for control retina; $p = 0.05005$) (h) Quantification of GFAP ($D_f = 5$; $t$-value = 5.91; $n = 3$ for ROP retina; $n = 4$ for control retina; $p = 0.0101$). ELM – External Limiting Membrane; ONL – Outer Nuclear Layer; OPL – Outer Plexiform Layer; INL – Inner Nuclear Layer; IPL – Inner Plexiform Layer; GCL – Ganglion Cell Layer; NFL – Nerve Fiber Layer; BV– Blood Vessels. The arrow shows blood vessels lining. The experiments were performed thrice with a similar protocol. A retinal section with no primary antibody was used as a negative control for normalization and human skin as a positive control for EPHX2 (Figure SF2). Scale: 20 µm; Magnification: 64X; Microscope: Carl Zeiss AG. Statistical significance is represented as * and ** for $p \leq 0.05$ and $p \leq 0.01$, respectively.

metabolic reprogramming, which could trigger an early onset of ROP, with the additional impact of oxidative insults (Szczuko et al., 2020). Placental genomics and RNA expression profiles are known to mediate genetic associations with complex health traits and diseases (Bhattacharya et al., 2022; Rasmussen et al., 2022). A detailed study by our group shows the involvement of maternal–fetal factors, placental histopathology, and molecular alterations related to hypoxia, inflammation, and complement activation at the maternal–fetal interface in preterm ROP placentas (Kaur et al., 2023). Retinas from ROP infants showed increased fibrosis, gliosis, cell proliferation, and an increased number of blood vessels (Figure 6). The different layers of the retina could not be distinguished in ROP infants because of a marked loss of photoreceptors and ganglion cells compared to the age-matched control retina. Further, EPHX2 was significantly downregulated in ROP retina, validating our findings on placental and blood gene expression at severe ROP. We also observed that there was no significant change in *EPHX2* expression (fold change: 1.02; $p$-value: 0.39; Figure S1) when the cohort was grouped on the

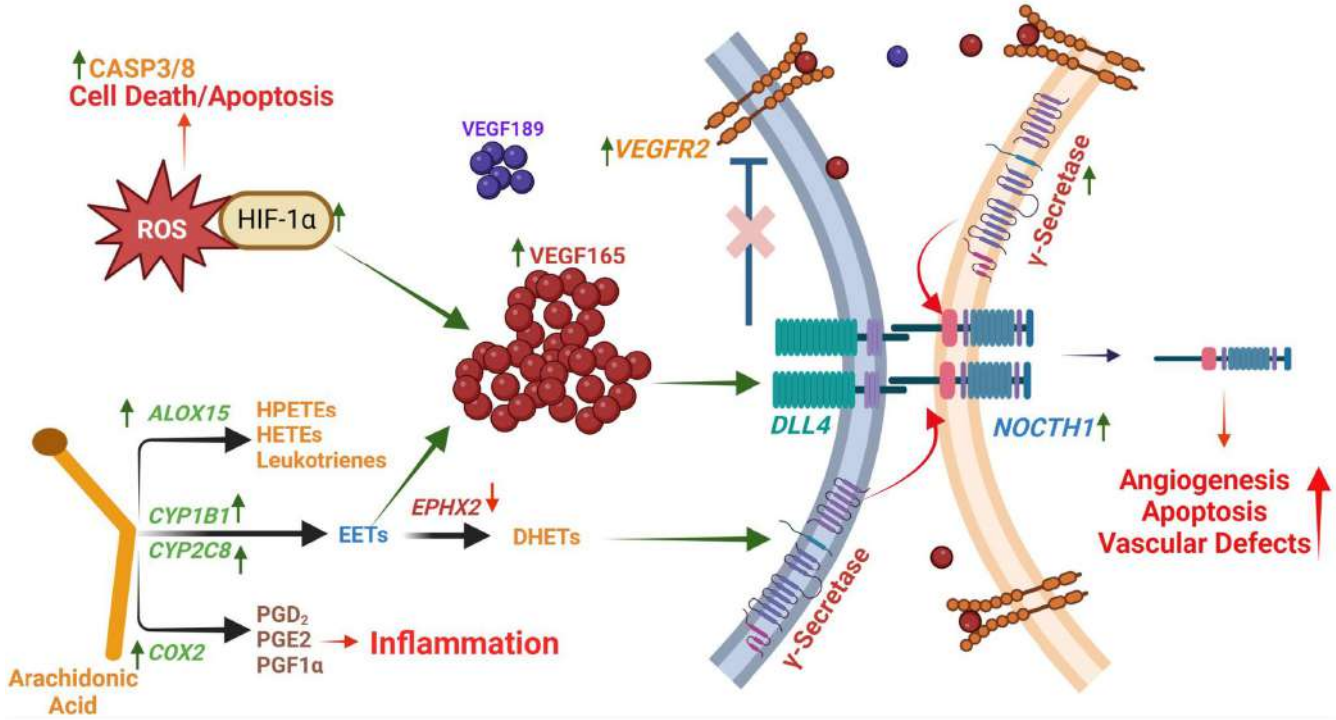


FIGURE 7 Schematic diagram of the mechanism of the proposed hypothesis of AA-metabolizing enzymes and its potential effect on angiogenesis, cell death, and inflammation.

basis of birth weight (birth weight: ≤1200 g; >1200 g). However, we believe post-birth weight gain among infants would play a significant role in its expression, which could not be studied because of the unavailability of the desired data from follow-ups. Our study cohort included infants with different treatments and duration of treatment, which could have an impact on the study results; however, this will be confirmed by further functional validation in an appropriate animal model. Further validation of the gene expression across different stages of ROP would have been ideal for studying a severity-dependent change in lipid-metabolizing enzymes and their activity; however, this was not possible because of the non-availability of VH samples from mild ROP. Astrocytes and other glial cells express *EPHX2* in the retina, thus performing a comparative expression of *EPHX2* across different cell types among cases and controls by immunostaining could have helped in distinguishing its diseased vs normal state, but this too could not be done because of the non-availability of the retina in normal pediatric donors. Nevertheless, notwithstanding these limitations, the study still very clearly demonstrated the involvement of fatty acid (PUFAs)-metabolizing enzymes in ROP, from placental to retinal changes. A major limitation of the present study is that the absolute quantification of most of the metabolites could not be performed as LC-MS/MS fragmentation could not be curated. However, adducts were analyzed in both positive and negative modes to exclude isobaric lipids. The absolute levels of some other prominent lipid metabolites could not be elucidated, as these did not qualify the threshold of 15 ppm mass tolerance. These are warranted in future studies to clearly establish their role in ROP pathogenesis.

## 5 | CONCLUSIONS

In summary, a systematic correlation of the expression of lipid-metabolizing enzymes in the AA pathway and their activity with the genes involved in angiogenesis as seen in severe ROP patients (present study) confirmed that altered lipid metabolism leading to pro-inflammatory conditions could be a potential mediator of neovascularization in the eyes of infants with severe ROP (Figure 7). The findings of this study would aid in discovering lipid-based biomarkers and therapeutics for prognostic testing and detecting newer drug targets for efficient management of ROP. This study can further be extended to study the response of mothers to ω-3 fatty acid supplementation during the prenatal and early postnatal stages to identify the infants who would benefit from this treatment. A recent clinical study showed improved visual acuity among ROP infants with ω-3 fatty acid supplementation (Lundgren et al., 2023). Identifying and treating the disease at an early onset stage would certainly help in the appropriate and effective management of the disease and its progression.

### AUTHOR CONTRIBUTIONS

**Saurabh Kumar:** Conceptualization; methodology; writing – original draft; validation; software; data curation; formal analysis; investigation. **Satish Patnaik:** Methodology; software; data curation; validation; writing – original draft. **Manjunath B. Joshi:** Formal analysis; data curation; supervision; writing – review and editing; methodology. **Neha Sharma:** Data curation; methodology. **Tarandeep Kaur:** Data curation; methodology. **Subhadra Jalali:** Investigation; writing – review and editing; supervision.

**Ramesh Kekunnaya:** Investigation; writing – review and editing. **Subhabrata Chakrabarti:** Supervision; formal analysis; writing – review and editing. **Inderjeet Kaur:** Conceptualization; methodology; data curation; supervision; resources; project administration; validation; visualization; writing – review and editing; writing – original draft; funding acquisition; investigation.

## ACKNOWLEDGMENTS

The authors thank the parents of all the preterm and full-term babies for their voluntary participation. We also thank Ms Udaya Chandrika and Mr. Tirupati Rao Mocherla, technical associates at Central Instrumentation Facility, BHERC, LVPEI for their support in performing Confocal microscopy and Cryosectioning of retina specimens, respectively.

## FUNDING INFORMATION

This work was partly supported by a COE grant (BT/PR32404/MED/30/2136/2019) from the Department of Biotechnology, IMPRINT grant (IMP/2018/001414) from the Ministry of Human Resource and development-Department of Science and Technology-Govt. of India, and Hyderabad Eye Research Foundation. SK is supported through the Department of Biotechnology, Government of India fellowship (DBT/2020/LVPEI/1365). NS is supported through the Department of Science and Technology-INSPIRE Fellowship (IF190699). AM is supported through the DBT India Alliance grant (no: IA/E/22/1/506766).

## CONFLICT OF INTEREST STATEMENT

The authors declare that there is no conflict of interest regarding the publication of this paper.

## PEER REVIEW

The peer review history for this article is available at https://www.webofscience.com/api/gateway/wos/peer-review/10.1111/jnc.16190.

## DATA AVAILABILITY STATEMENT

All data generated or analyzed during this study are included in this published article and is available upon request. The Preprint of this article was posted on BioRXiv, May 16th 2022; https://www.biorxiv.org/content/10.1101/2022.05.13.491711v1.full.pdf.

## ORCID

*Saurabh Kumar* https://orcid.org/0000-0002-6929-0830
*Aatish Mahajan* https://orcid.org/0000-0002-5064-6921
*Subhabrata Chakrabarti* https://orcid.org/0000-0003-3717-4963
*Inderjeet Kaur* https://orcid.org/0000-0003-3660-5039

## REFERENCES

Bhattacharya, A., Freedman, A. N., Avula, V., Harris, R., Liu, W., Pan, C., Lusis, A. J., Joseph, R. M., Smeester, L., Hartwell, H. J., Kuban, K. C. K., Marsit, C. J., Li, Y., O'Shea, T. M., Fry, R. C., & Santos, H. P., Jr. (2022). Placental genomics mediates genetic associations with complex health traits and disease. *Nature Communications*, *13*(1), 706. https://doi.org/10.1038/s41467-022-28365-x

Blencowe, H., Lawn, J. E., Vazquez, T., Fielder, A., & Gilbert, C. (2013). Preterm-associated visual impairment and estimates of retinopathy of prematurity at regional and global levels for 2010. *Pediatric Research*, *74*(1), 35–49.

Brunkan, A. L., & Goate, A. M. (2005). Presenilin function and gamma-secretase activity. *Journal of Neurochemistry*, *93*(4), 769–792.

Chen, J., & Smith, L. E. (2007). Retinopathy of prematurity. *Angiogenesis*, *10*(2), 133–140. https://doi.org/10.1007/s10456-007-9066-0

Cheranov, S. Y., Karpurapu, M., Wang, D., Zhang, B., Venema, R. C., & Rao, G. N. (2008). An essential role for SRC-activated STAT-3 in 14,15-EET-induced VEGF expression and angiogenesis. *Blood*, *111*(12), 5581–5591. https://doi.org/10.1182/blood-2007-11-126680

Dhyani, V., Kumar, S., Manne, S. R., Kaur, I., Jana, S., Russell, S., Sarkar, R., & Giri, L. (2023). Three-dimensional tracking of intracellular calcium and redox state during real-time control in a hypoxic gradient in microglia culture: Comparison of the channel blocker and reoxygenation under ischemic shock. *ACS Chemical Neuroscience*, *14*(10), 1810–1825. https://doi.org/10.1021/acschemneuro.2c00807

Diebold, L. P., Gil, H. J., Gao, P., Martinez, C. A., Weinberg, S. E., & Chandel, N. S. (2019). Mitochondrial complex III is necessary for endothelial cell proliferation during angiogenesis. *Nature Metabolism*, *1*(1), 158–171. https://doi.org/10.1038/s42255-018-0011-x

Dufour, M., Faes, S., Dormond-Meuwly, A., Demartines, N., & Dormond, O. (2014). PGE2-induced colon cancer growth is mediated by mTORC1. *Biochemical and Biophysical Research Communications*, *451*(4), 587–591. https://doi.org/10.1016/j.bbrc.2014.08.032

Fischer, A. H., Jacobson, K. A., Rose, J., & Zeller, R. (2008). Hematoxylin and eosin staining of tissue and cell sections. *CSH Protocols*, *2008*, pdb.prot4986. https://doi.org/10.1101/pdb.prot4986

Fu, Z., Yan, W., Chen, C. T., Nilsson, A. K., Bull, E., Allen, W., Yang, J., Ko, M., SanGiovanni, J. P., Akula, J. D., Talukdar, S., Hellström, A., & Smith, L. E. H. (2022). Omega-3/Omega-6 long-chain fatty acid imbalance in phase I retinopathy of prematurity. *Nutrients*, *14*(7), 1333. https://doi.org/10.3390/nu14071333

Garcia, A., & Kandel, J. J. (2012). Notch: A key regulator of tumor angiogenesis and metastasis. *Histology and Histopathology*, *27*(2), 151–156. https://doi.org/10.14670/HH-27.151

Gustafsson, M. V., Zheng, X., Pereira, T., Gradin, K., Jin, S., Lundkvist, J., Ruas, J. L., Poellinger, L., Lendahl, U., & Bondesson, M. (2005). Hypoxia requires notch signaling to maintain the undifferentiated cell state. *Developmental Cell*, *9*(5), 617–628. https://doi.org/10.1016/j.devcel.2005.09.010

Harris, T. R., & Hammock, B. D. (2013). Soluble epoxide hydrolase: gene structure, expression and deletion. *Gene*, *526*(2), 61–74. https://doi.org/10.1016/j.gene.2013.05.008

Harshitha, R., & Arunraj, D. R. (2021). Real-time quantitative PCR: A tool for absolute and relative quantification. *Biochemistry and Molecular Biology Education*, *49*(5), 800–812. https://doi.org/10.1002/bmb.21552

Hartmann, D., de Strooper, B., Serneels, L., Craessaerts, K., Herreman, A., Annaert, W., Umans, L., Lübke, T., Lena Illert, A., von Figura, K., & Saftig, P. (2002). The disintegrin/metalloprotease ADAM 10 is essential for Notch signalling but not for alpha-secretase activity in fibroblasts. *Human Molecular Genetics*, *11*(21), 2615–2624. https://doi.org/10.1093/hmg/11.21.2615

Hartnett, M. E. (2015). Pathophysiology and mechanisms of severe retinopathy of prematurity. *Ophthalmology*, *122*(1), 200–210. https://doi.org/10.1016/j.ophtha.2014.07.050

Hartnett, M. E., & Lane, R. H. (2013). Effects of oxygen on the development and severity of retinopathy of prematurity. *Journal of AAPOS*, *17*(3), 229–234. https://doi.org/10.1016/j.jaapos.2012.12.155

Hellström, M., Phng, L. K., & Gerhardt, H. (2007). VEGF and notch signaling: The yin and yang of angiogenic sprouting. *Cell Adhesion & Migration*, *1*(3), 133–136. https://doi.org/10.4161/cam.1.3.4978

Hou, H. H., Hammock, B. D., Su, K. H., Morisseau, C., Kou, Y. R., Imaoka, S., Oguro, A., Shyue, S. K., Zhao, J. F., & Lee, T. S. (2012). N-terminal domain of soluble epoxide hydrolase negatively regulates the VEGF-mediated activation of endothelial nitric oxide synthase. *Cardiovascular Research*, *93*(1), 120–129. https://doi.org/10.1093/cvr/cvr267

Hu, J., Bibli, S. I., Wittig, J., Zukunft, S., Lin, J., Hammes, H. P., Popp, R., & Fleming, I. (2019). Soluble epoxide hydrolase promotes astrocyte survival in retinopathy of prematurity. *The Journal of Clinical Investigation*, *129*(12), 5204–5218.

Hu, J., Dziumbla, S., Lin, J., Bibli, S. I., Zukunft, S., de Mos, J., Awwad, K., Frömel, T., Jungmann, A., Devraj, K., Cheng, Z., Wang, L., Fauser, S., Eberhart, C. G., Sodhi, A., Hammock, B. D., Liebner, S., Müller, O. J., Glaubitz, C., … Fleming, I. (2017). Inhibition of soluble epoxide hydrolase prevents diabetic retinopathy. *Nature*, *552*(7684), 248–252. https://doi.org/10.1038/nature25013

Hu, J., Popp, R., Frömel, T., Ehling, M., Awwad, K., Adams, R. H., Hammes, H. P., & Fleming, I. (2014). Müller glia cells regulate notch signaling and retinal angiogenesis via the generation of 19,20-dihydroxydocosapentaenoic acid. *The Journal of Experimental Medicine*, *211*(2), 281–295. https://doi.org/10.1084/jem.20131494

Kaur, T., Patnaik, S., Kumar, S., & Kaur, I. (2022). Molecular mechanisms in the pathogenesis of retinopathy of prematurity (ROP). In H. V. Nema & N. Nema (Eds.), *Genetics of ocular diseases*. Springer. https://doi.org/10.1007/978-981-16-4247-0_9

Kaur, T., Sharma, N., Jakati, S., Bagga, N., Mitra, S., Bhargavi, K., Jalali, S., & Kaur, I. (2023). *Role of maternal, fetal and placental histopathology factors in the pathogenesis of retinopathy of prematurity*. bioRxiv.02.13.528236.

Kopan, R., & Ilagan, M. X. (2009). The canonical notch signaling pathway: Unfolding the activation mechanism. *Cell*, *137*(2), 216–233. https://doi.org/10.1016/j.cell.2009.03.045

Kumar, S., Joshi, M. B., & Kaur, I. (2023). Protocol and methods applicable to retinal vascular diseases. *Methods in Molecular Biology*, *2625*, 71–78. https://doi.org/10.1007/978-1-0716-2966-6_6

Lapillonne, A., & Moltu, S. J. (2016). Long-chain polyunsaturated fatty acids and clinical outcomes of preterm infants. *Annals of Nutrition & Metabolism*, *69*(Suppl 1), 35–44.

Liu, A., Terry, R., Lin, Y., Nelson, K., & Bernstein, P. S. (2013). Comprehensive and sensitive quantification of long-chain and very long-chain polyunsaturated fatty acids in small samples of human and mouse retina. *Journal of Chromatography. A*, *1307*, 191–200.

Lobov, I. B., Renard, R. A., Papadopoulos, N., Gale, N. W., Thurston, G., Yancopoulos, G. D., & Wiegand, S. J. (2007). Delta-like ligand 4 (Dll4) is induced by VEGF as a negative regulator of angiogenic sprouting. *Proceedings of the National Academy of Sciences of the United States of America*, *104*(9), 3219–3224. https://doi.org/10.1073/pnas.0611206104

Lundgren, P., Jacobson, L., Gränse, L., Hård, A. L., Sävman, K., Hansen-Pupp, I., Ley, D., Nilsson, A. K., Pivodic, A., Smith, L. E., & Hellström, A. (2023). Visual outcome at 2.5 years of age in $\omega$-3 and $\omega$-6 long-chain polyunsaturated fatty acid supplemented preterm infants: A follow-up of a randomized controlled trial. *Lancet Regional Health—Europe*, *32*, 100696. https://doi.org/10.1016/j.lanepe.2023.100696

Luo, J., Feng, X. X., Luo, C., Wang, Y., Li, D., Shu, Y., Wang, S. S., Qin, J., Li, Y. C., Zou, J. M., Tian, D. A., Zhang, G. M., & Feng, Z. H. (2016). 14,15-EET induces the infiltration and tumor-promoting function of neutrophils to trigger the growth of minimal dormant metastases. *Oncotarget*, *7*(28), 43324–43336. https://doi.org/10.18632/oncotarget.9709

Morisseau, C., & Hammock, B. D. (2013). Impact of soluble epoxide hydrolase and epoxyeicosanoids on human health. *Annual Review of Pharmacology and Toxicology*, *53*, 37–58. https://doi.org/10.1146/annurev-pharmtox-011112-140244

Naeem, Z., Zukunft, S., Huard, A., Hu, J., Hammock, B. D., Weigert, A., Frömel, T., & Fleming, I. (2024). Role of the soluble epoxide hydrolase in keratinocyte proliferation and sensitivity of skin to inflammatory stimuli. *Biomedicine & Pharmacotherapy*, *171*, 116127. https://doi.org/10.1016/j.biopha.2024.116127

Nguyen, C. H., Stadler, S., Brenner, S., Huttary, N., Krieger, S., Jäger, W., Dolznig, H., & Krupitza, G. (2016). Cancer cell-derived 12(S)-HETE signals via 12-HETE receptor, RHO, ROCK and MLC2 to induce lymph endothelial barrier breaching. *British Journal of Cancer*, *115*(3), 364–370. https://doi.org/10.1038/bjc.2016.201

Patnaik, S., Jalali, S., Joshi, M. B., Satyamoorthy, K., & Kaur, I. (2019). Metabolomics applicable to retinal vascular diseases. *Methods in Molecular Biology*, *1996*, 325–331. https://doi.org/10.1007/978-1-4939-9488-5_24

Patnaik, S., Rai, M., Jalali, S., Agarwal, K., Badakere, A., Puppala, L., Vishwakarma, S., Balakrishnan, D., Rani, P. K., Kekunnaya, R., Chhablani, P. P., Chakrabarti, S., & Kaur, I. (2021). An interplay of microglia and matrix metalloproteinase MMP9 under hypoxic stress regulates the opticin expression in retina. *Scientific Reports*, *11*, 7444. https://doi.org/10.1038/s41598-021-86302-2

Rand, A. A., Rajamani, A., Kodani, S. D., Harris, T. R., Schlatt, L., Barnych, B., Passerini, A. G., & Hammock, B. D. (2019). Epoxyeicosatrienoic acid (EET)-stimulated angiogenesis is mediated by epoxy hydroxyeicosatrienoic acids (EHETs) formed from COX-2. *Journal of Lipid Research*, *60*(12), 1996–2005. https://doi.org/10.1194/jlr.M094219

Rasmussen, M., Reddy, M., Nolan, R., Camunas-Soler, J., Khodursky, A., Scheller, N. M., Cantonwine, D. E., Engelbrechtsen, L., Mi, J. D., Dutta, A., Brundage, T., Siddiqui, F., Thao, M., Gee, E. P. S., Ia, J., Baruch-Gravett, C., Santillan, M. K., Deb, S., Ame, S. M., … McElrath, T. F. (2022). RNA profiles reveal signatures of future health and disease in pregnancy. *Nature*, *601*(7893), 422–427. https://doi.org/10.1038/s41586-021-04249-w

Rathi, S., Jalali, S., Patnaik, S., Shahulhameed, S., Musada, G. R., Balakrishnan, D., Rani, P. K., Kekunnaya, R., Chhablani, P. P., Swain, S., Giri, L., Chakrabarti, S., & Kaur, I. (2017). Abnormal complement activation and inflammation in the pathogenesis of retinopathy of prematurity. *Frontiers in Immunology*, *8*, 1868. https://doi.org/10.3389/fimmu.2017.01868

Rivera, J. C., Holm, M., Austeng, D., Morken, T. S., Zhou, T. E., Beaudry-Richard, A., Sierra, E. M., Dammann, O., & Chemtob, S. (2017). Retinopathy of prematurity: Inflammation, choroidal degeneration, and novel promising therapeutic strategies. *Journal of Neuroinflammation*, *14*(1), 165. https://doi.org/10.1186/s12974-017-0943-1

Sanghi, G., Narang, A., Narula, S., & Dogra, M. R. (2018). WINROP algorithm for prediction of sight threatening retinopathy of prematurity: Initial experience in Indian preterm infants. *Indian Journal of Ophthalmology*, *66*(1), 110–113.

Shahulhameed, S., Vishwakarma, S., Chhablani, J., Tyagi, M., Pappuru, R. R., Jakati, S., Chakrabarti, S., & Kaur, I. (2020). A systematic investigation on complement pathway activation in diabetic retinopathy. *Frontiers in Immunology*, *11*, 154. https://doi.org/10.3389/fimmu.2020.00154

Snodgrass, R. G., & Brune, B. (2019). Regulation and functions of 15-lipoxygenases in human macrophages. *Frontiers in Pharmacology*, *10*, 719.

Sorensen, E. B., & Conner, S. D. (2010). $\gamma$-Secretase-dependent cleavage initiates notch signaling from the plasma membrane. *Traffic*, *11*(9), 1234–1245. https://doi.org/10.1111/j.1600-0854.2010.01090.x

Spector, A. A., & Norris, A. W. (2007). Action of epoxyeicosatrienoic acids on cellular function. *American Journal of Physiology. Cell Physiology*, *292*(3), C996–C1012. https://doi.org/10.1152/ajpcell.00402.2006

Szczuko, M., Kikut, J., Komorniak, N., Bilicki, J., Celewicz, Z., & Ziętek, M. (2020). The role of arachidonic and linoleic acid derivatives in pathological pregnancies and the human reproduction process. *International Journal of Molecular Sciences*, *21*(24), 9628. https://doi.org/10.3390/ijms21249628

Toms, A. S., & Rai, E. (2019). Operative fasting guidelines and postoperative feeding in paediatric anaesthesia-current concepts. *Indian Journal of Anaesthesia*, *63*(9), 707–712. https://doi.org/10.4103/ija.IJA_484_19

Wang, T., Fu, X., Chen, Q., Patra, J. K., Wang, D., Wang, Z., & Gai, Z. (2019). Arachidonic acid metabolism and kidney inflammation. *International Journal of Molecular Sciences*, *20*(15), 3683. https://doi.org.10.3390/ijms20153683

Wang, B., Wu, L., Chen, J., Dong, L., Chen, C., Wen, Z., Hu, J., Fleming, I., & Wang, D. W. (2021). Metabolism pathways of arachidonic acids: Mechanisms and potential therapeutic targets. *Signal Transduction and Targeted Therapy*, *6*(1), 94. https://doi.org/10.1038/s41392-020-00443-w

Webler, A. C., Michaelis, U. R., Popp, R., Barbosa-Sicard, E., Murugan, A.Falck, J. R., Fisslthaler, B., & Fleming, I. (2008). Epoxyeicosatrienoic acids are part of the VEGF-activated signaling cascade leading to angiogenesis. *American Journal of Physiology. Cell Physiology*, *295*(5), C1292–C1301. https://doi.org/10.1152/ajpcell.00230.2008

Welch, W. J., Patel, K., Modlinger, P., Mendonca, M., Kawada, N., Dennehy, K., Aslam, S., & Wilcox, C. S. (2007). Roles of vasoconstrictor prostaglandins, COX-1 and -2, and AT1, AT2, and TP receptors in a rat model of early 2K,1C hypertension. *American Journal of Physiology. Heart and Circulatory Physiology*, *293*(5), H2644–H2649.

Zemski Berry, K. A., Gordon, W. C., Murphy, R. C., & Bazan, N. G. (2014). Spatial organization of lipids in the human retina and optic nerve by MALDI imaging mass spectrometry. *Journal of Lipid Research*, *55*(3), 504–515.

Zhou, Z., Reddy, K., Guan, H., & Kleinerman, E. S. (2007). VEGF(165), but not VEGF(189), stimulates vasculogenesis and bone marrow cell migration into Ewing's sarcoma tumors in vivo. *Molecular Cancer Research*, *5*(11), 1125–1132.

## SUPPORTING INFORMATION

Additional supporting information can be found online in the Supporting Information section at the end of this article.

**How to cite this article:** Kumar, S., Patnaik, S., Joshi, M. B., Sharma, N., Kaur, T., Jalali, S., Kekunnaya, R., Mahajan, A., Chakrabarti, S., & Kaur, I. (2024). Arachidonic acid metabolism regulates the development of retinopathy of prematurity among preterm infants. *Journal of Neurochemistry*, *00*, 1–17. https://doi.org/10.1111/jnc.16190